journal of the international meteor organization

WGN

40:4
august 2012

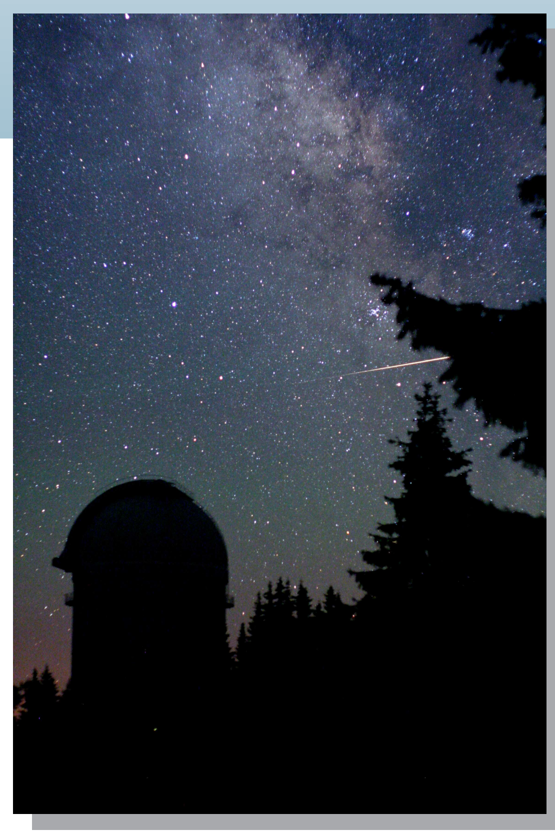

Draconids
Three components of Taurids
April–May video meteors

ISSN 1016-3115

WGN Vol. 40, No. 4, August 2012, pp. 113 – 148

Administrative

Draconids

Meteor science

Preliminary results

Front cover photo

A fireball photographed on 2012 June 19 at 22^h24^m UT from the National Astronomical Observatory NAO Rozhen, Bulgaria. Canon 350D camera equipped with Takumar 50 mm f/1.4 lens used at f/2 was employed for this 25 s exposure at ISO 1600. A controversial spiral trajectory of the fireball can be seen in full-resolution photo. Photo courtesy: Pencho Markishky.

Writing for WGN

This Journal welcomes papers submitted for publication. All papers are reviewed for scientific content, and edited for English and style. Instructions for authors can be found in WGN **31:4**, 124–128, and at `http://www.imo.net/articles/writingforwgn.pdf` .

Cover design

Rainer Arlt

Legal address

International Meteor Organization, Mattheessensstraat 60, 2540 Hove, Belgium.

Editorial

Javor Kac

There is a Perseid observing recollection and an anticipation of the coming IMC that I want to share with you this time.

Perseids

After months of meteor observing abstinence I finally got a chance for some serious observing in August. I have spent ten delightful days at the youth astronomical research camp in Medvedje brdo, Slovenia. I could observe on all nine nights at the camp. Although many of them were not perfectly clear, this is probably a record span of consecutive observing nights at such camps in the last two decades.

Adding one more observing night after the camp, I observed for almost 43 hours and recorded 1112 meteors in August. As the camp was organized around the Perseid peak, most shower meteors seen were the Perseids (673), with other showers represented by 116 meteors along with 323 sporadics.

Preliminary results of the worldwide effort (`http://www.imo.net/live/perseids2012/`) indicate a maximum on August 12, probably during European daytime hours.

Hopefully I will have more opportunities for meteor observing in the rest of the year. I am especially looking forward to the Taurids, Orionids and Geminids.

International Meteor Conference

In just a couple of weeks, the 31st International Meteor Conference is going to take place on La Palma. Having a conference at such a venue will be a great opportunity to combine the event with some sightseeing and observing. This will be my first visit to the Canary Islands, and I am looking forward to exploring geology, flora and fauna of this region. I am also excited to visit the world-famous observatory and I hope we will have a chance to observe from the top of the mountain. Of course, all these experiences are going to be spiced up by the traditionally pleasant atmosphere that the IMC is offering.

In this issue

This issue of WGN is quite a thick one. A series of the 2011 Draconid outburst reports and analyses is presented. Toth et al. present their double-station observation results with 43 Draconid orbits; Sarneczky and Igaz, and Vandeputte share their personal experience of the outburst as observed from Slovenia and Portugal, respectively; and McBeath presents the radio results of the maximum. Next, Koseki describes his findings about the three components of the Taurids. Finally, regular reports of the IMO Video Meteor Network observations for April and May are presented.

I believe you are going to enjoy the works presented.

IMO bibcode WGN-404-editorial NASA-ADS bibcode 2012JIMO...40Q.113K

Call for photographs

Javor Kac

We are frequently short of photographs for the *WGN* covers that we publish in colour (front cover) or black&white (back cover). If you think you have a suitable meteor-related photograph, please offer it to us. More or less any computer image format will do. You can send your photographs to `wgn@imo.net`, but remember to put 'Meteor' in the subject line to get round the anti-spam filters.

IMO bibcode WGN-404-kac-call NASA-ADS bibcode 2012JIMO...40R.113K

Sir Bernard Lovell (1913 – 2012)

Megan Argo

Received 2012 August 20

Sir Bernard Lovell, founder and first Director of Jodrell Bank Observatory in Cheshire, died on 6th August 2012 at the age of 98. Sir Bernard, Emeritus Professor of Radioastronomy at The University of Manchester, was one of the pioneers of radio meteor astronomy and the man behind the iconic 76-metre Mark I telescope at Jodrell Bank, later renamed in his honour on the occasion of its 30th anniversary.

Born in 1913 in Oldland Common, Gloucestershire, Sir Bernard studied at the University of Bristol before moving to Manchester in 1936 to work in the Department of Physics. During the Second World War Sir Bernard led the team that developed H2S radar, work for which he was later awarded the OBE. Noticing that the radar operators ignored certain types of echoes on their screens, knowing that they were not caused by aircraft, he resolved to investigate the nature of these natural reflections once the war was over.

Sir Bernard returned to Manchester in 1945 and continued his pre-war research on cosmic ray air showers. Through his contacts in the military, he acquired some unwanted 4-metre radar equipment which he initially set up near the physics department in the city. His hope was that the mysterious echoes notice by the wartime radar operators were caused by cosmic rays. At that time Oxford Road, one of the main routes into the city, included a busy electric tram line. Locating the equipment in a university quadrangle, Lovell quickly realised that the interference caused by the direct current needed to operate the nearby tram line was so strong as to render the radar equipment completely useless. Then, in late 1945, Lovell took his equipment to the University's botanical station at Jodrell Bank in Cheshire, founding what would later become the world-famous Observatory.

Today, the site is dominated by the 76-metre Lovell Telescope, a giant metal eye on the sky sticking up out of the Cheshire plain, an icon of British science and engineering visible for many miles around and inspiring countless thousands of school children to this day. Sir Bernard worked with engineer Sir Charles Husband to build the telescope which was by far the world's largest when it was completed in 1957; within days of its completion the telescope was used to track the carrier rocket which took Sputnik 1 into orbit, marking the dawn of the space age. The telescope was, at that time, the only instrument in the world capable of tracking ballistic rockets, and the successful tracking of the Sputnik rockets saved the Observatory from closure and Lovell himself from the threat of prison. The Mark I is still the third largest fully-steerable telescope in the world and a series of upgrades mean it is now more capable than ever, observing and discovering many phenomena undreamed of when it was first conceived.

Figure 1 – Sir Bernard Lovell, founder of Jodrell Bank Observatory, led the team that developed H2S radar during WWII and was knighted in 1961 for his pioneering work in radio astronomy at Manchester University. Credit: Jodrell Bank Centre for Astrophysics, University of Manchester.

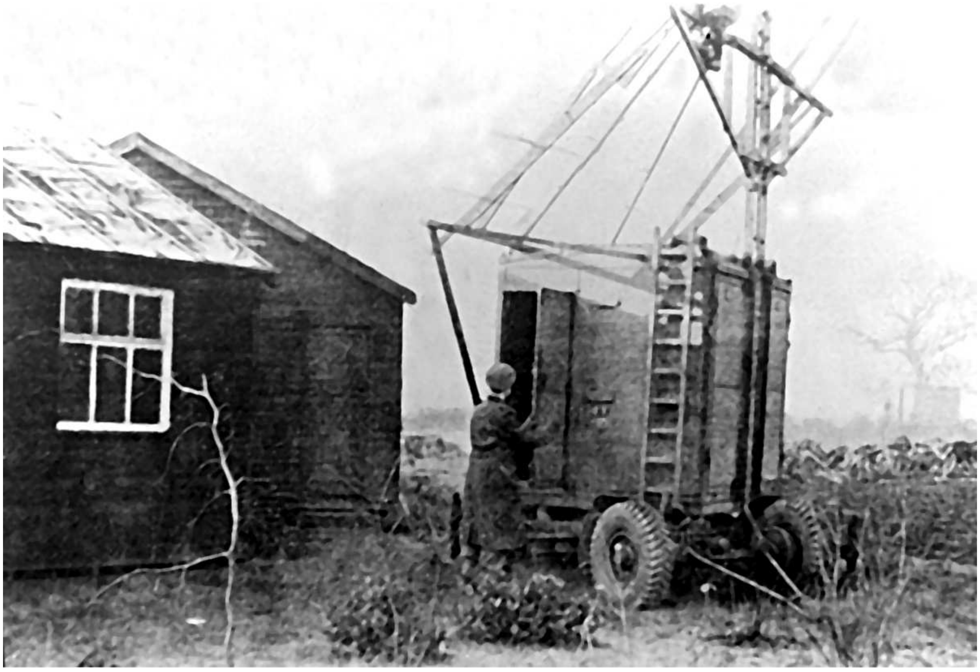

Figure 2 – December 1945 in the Botanical Grounds - the first observations at Jodrell Bank. Credit: Jodrell Bank Centre for Astrophysics, University of Manchester.

While the very early days of astronomy at Jodrell Bank Experimental Station were no less important, they were far less glamorous. When Lovell and a small group first arrived on the site in 1945 with a couple of trailers of ex-military radar gear, the first observing site was chosen more because one of the vehicles became stuck in the Cheshire mud, rather than for its suitability as an observing location. Known as the Park Royal, the vehicle served as the observing headquarters for the early meteor work and later gave its name to the control building for the Mark II telescope, constructed nearby in 1964.

One of the meteor showers observed in the early days from the Park Royal trailer was the Giacobinid storm of October 1946. Having rigged up a series of yagis on an old searchlight mount such that the beam could be steered anywhere on the sky, Lovell and his colleagues observed the storm throughout the night at a wavelength of 4.2 metres. In Lovell's own words: "It was as though one was being showered from space with vast numbers of missiles, which suddenly disappeared before one's eyes as they burnt up in the high atmosphere." Around the maximum, visual rates at Jodrell were around 4000 per hour, and the echoes on the radar tube were too numerous to count, so instead they ran a camera to photograph the screen in order to analyse the results later. The records showed that the radio rate was almost 10 000 per hour, peaking at 168 meteors per minute. During this period of intense meteor activity they carried out another important experiment. With the beam of the antenna array at 90 degrees to the radiant the echoes on the cathode ray tube were too numerous to count, but when they turned the yagis so that the beam was directly towards the radiant the count rate collapsed instantly. This proved that the echoes the radar operators had first seen during the war were, in fact, radar reflections from meteor trails in the ionosphere, not from some other atmospheric phenomenon.

In the years before construction of the Mark I telescope began in 1952, the Jodrell group, under Lovell's leadership, carried out significant research in the field of radio meteors, answering several important questions of the day. One problem at the time was the nature of sporadic meteors. There was some debate, often heated, among researchers in the field as to whether such meteors were confined to the solar system, or were on hyperbolic orbits and hence interstellar in nature. It was realised that if the velocity of such sporadic meteors could be determined then the question could be definitively answered, so Lovell and his colleagues set about doing just that. Because of the way the Earth moves in its orbit around the Sun, the maximum velocity you would expect to observe from meteors confined to the solar system is 72 kilometres per second. Over several years, with antennas of increasing sensitivity, the group measured the velocities of sporadic meteors down to magnitude +8 and found no evidence whatsoever of any with hyperbolic velocities, finally settling the argument.

Another important line of research carried out by Lovell's group in the early days made use of the steerable array of yagis. Using this array, the sky position of a shower's radiant could be determined since (as found during the Giacobinids) when the yagis were pointed at this location, the count rate would drop to zero. Using this setup, together with an ingenious automated recording system, the group were able to confirm the radiants of all the major known showers at the time. They also discovered, much to their amazement, that during the quiet season between the Lyrids in April and the Perseids in August, there were unexpected periods of intense activity which had never been observed by eye. The reason being, of course, that these streams were active only during daylight and so could never be observed visually.

Meteor research continued once construction of the Mark I telescope began, but other fields of study became increasingly important as techniques improved and telescopes began to increase in both sensitivity and resolution. Today the Lovell Telescope plays a key role in world-leading research on pulsars, testing our understanding of extreme physics including Einstein's General Theory of Relativity, while the Observatory as a whole continues to play a major role in astronomical research. Jodrell Bank is home to the e-MERLIN array, seven radio telescopes spread across the UK which can match at radio wavelengths the resolution of the Hubble telescope in the optical. Based on the techniques of linking telescopes over long distances pioneered by the team which Sir Bernard assembled at Jodrell Bank, the e-MERLIN telescopes are now connected by a high-speed optical fibre network making it one of the most powerful telescope arrays in the world. The Lovell telescope is also an important member of the European Very Long Baseline Interferometry Network which connects telescopes across many countries to produce an array of superb sensitivity and resolution. Later in 2012 the international headquarters of the SKA Organisation will move to Jodrell Bank. The Square Kilometre Array (SKA) will be the world's largest telescope, combining thousands of dishes and other receivers spread across thousands of kilometres in both southern Africa and Australia.

Sir Bernard made important contributions to many fields of research, played a vital role in the second world war, was responsible for construction of the Jodrell Bank telescopes and authored an impressive collection of books and research papers, but his contributions to science stretch much wider. Over the last seven decades, many hundreds of scientists and engineers have worked and trained at Jodrell Bank, often going on to work at other observatories across the world. Jodrell Bank has also inspired generations of school children who have visited the Observatory, Sir Bernard recognised the enormous public interest in the telescope very early on and constructed a dedicated visitor centre on the site, one of the first public science centres in the world.

Sir Bernard is survived by four of his five children, fourteen grandchildren and fourteen great-grandchildren. In person, Sir Bernard was warm and generous and took a keen interest in goings on at the Observatory long after his retirement, continuing to come in to work at the Observatory until quite recently when ill health intervened. Outside the world of science he was an accomplished musician, playing the organ at the Swettenham Church for many years. He was also a keen cricketer, captain of the Chelford Cricket Club and past President of the Lancashire County Cricket Club. He was also renowned internationally for his passion for arboriculture, creating arboretums at both The Quinta and Jodrell Bank itself.

Sir Bernard's legacy is immense, extending from his wartime work to his pioneering contributions to radio astronomy and including his dedication to education and public engagement with scientific research. A great man, he will be sorely missed.

Further reading

Sir Bernard wrote many books about Jodrell Bank and astronomy in general, notable amongst these being 'The Story of Jodrell Bank' published in 1968 which details the early days at the botany station and the construction of the Mark I telescope. Follow up volumes (Out of the Zenith and The Jodrell Bank Telescopes) detail the later history of the observatory, including the development of MERLIN, an array of telescopes across the country which still operates today. His books also include 'Astronomer by Chance' which provides more of a personal account of his life and the circumstances which turned him towards a career in the new and rapidly-developing field of radio astronomy. He also authored many scientific papers and books, many of which can be found by searching the archives of Nature, Google Books, and `archive.org`. His scholarly works include 'Meteor Astronomy' which, written in 1954, was the definitive work in the field for some time.

In 1958, Sir Bernard presented the BBC Reith Lectures on 'The Individual and the Universe', and in 2008 he was interviewed on video for the Web of Stories. The videos are all archived and available online. In 2007, the year of the 50th anniversary of the completion of the Lovell telescope, a series of audio interviews with Sir Bernard were broadcast on the Jodcast, an astronomy podcast produced by students and postdocs at the University of Manchester.

IMO bibcode WGN-404-argo-lovell NASA-ADS bibcode 2012JIMO...40..114A

Draconids

Video observation of Draconids 2011 from Italy

Juraj Tóth[1], *Roman Piffl*[2], *Jakub Koukal*[2], *Przemysław Żołądek*[3], *Mariusz Wiśniewski*[3], *Štefan Gajdoš*[1], *Ferruccio Zanotti*[4], *Diego Valeri*[4], *Paolo De Maria*[4], *Martin Popek*[2], *Sylvie Gorková*[2], *Jozef Világi*[1], *Leonard Kornoš*[1], *Dušan Kalmančok*[1] *and Pavol Zigo*[1]

The joint observation of Draconids 2011 by one all-sky video camera of the Slovak Video Meteor Network (SVMN), cameras of the Central European Meteor Network (CEMeNt), the Polish Fireball Network and local Italian Meteor and TLE Network in the night of October 8–9 brought hundreds of detected meteors over Italy. Due to the problematic weather situation in Central Europe, several groups had to move up and locate their video equipment in the Northern Italy to become a part of a ground-based observational Draconids 2011 campaign. This enthusiasm and effort resulted in valuable observations, of which results are presented in this brief paper.

Received 2012 January 20

1 Introduction

The Draconid meteor shower belongs to established low level annual meteor showers, which are capable of producing outbursts or even meteor storms. The parent comet 21P/Giacobini-Zinner was discovered in 1900 and following dust ejecta modeling showed a possible outburst in activity on 2011 October 8 (Watanabe & Sato, 2008; Vaubaillon et al., 2011). The Draconids are one of the slowest meteor streams and the most fragile material (Borovička et al., 2007). An observational campaign from air and ground was needed. Due to uncertain weather conditions in Central Europe, several groups of observers have moved to Northern Italy, among them also the members of the Slovak Video Meteor Network (SVMN – Comenius University Bratislava) and of the Central European Meteor Network (CEMeNt – an amateur network consisting of several observers from the Czech Republic and Slovak Republic) and also members of the Polish Fireball Network (PFN). Later, common video meteors were identified also from the local Italian Meteor and TLE Network (IMTN).

2 Observations

We set up double-station observation performed by one all-sky video camera developed and constructed at the Astronomical and Geophysical Observatory in Modra (SVMN) and three video cameras of the CEMeNt network. The equipment of SVMN and CEMeNt was described in Tóth et al. (2008, 2011a, 2011b). The first station was located near the town Bettola (44°.7948 N, 9°.6244 E), the second one close to the village of Cavandola (44°.5658 N, 10°.4652 E) at a distance of 71 km east from the first station. Independently, double-station video observations were set up from PFN in location

Figure 1 – Location of ground-based video meteor stations of the SVMN, CEMeNt, PFN and IMTN in Northern Italy during the Draconids 2011.

Nogara (45°.1569 N, 11°.0925 E) and the second station close to the town of Bettolino di Novellara (44°.8864 N, 10°.7750 E) 39 km to the south-west from Nogara. Local Italian video stations of the IMTN, where we were able to find common meteors were located at Cuneo Associazione Astrofili Bisalta (44°.3957 N, 7°.5174 E), Fanano (Modena) (44°.2120 N, 10°.7559 N), Contigliano (Rieti) (42°.41141 N, 12°.7682 E), Tortoreto (Teramo) (13°.9350 E, 42°.8075 N) and Ferrara (44°.8181 N, 11°.6167 E). Visual observations were performed from the station of Cavandola. In total, there were 9 stations with 14 cameras participating on this joint campaign. The location of stations is shown in Figure 1.

3 Detection and data reduction

Video signals from the majority of cameras were detected by the UFOCapture software (SonotaCo, 2009), which is able to recognize meteors and bolides from camera analogue or digital signal. The meteor data were astrometrically analyzed by each experienced observer by using the UFOAnalyzer (SonotaCo, 2009) and the data from two Polish stations were recorded and analyzed by the Metrec software (Molau, 1999). These data were later transformed to the UFOOrbit format. The following results were obtained by the UFOOrbit software (SonotaCo, 2009). The meteor

[1]Faculty of Mathematics, Physics and Informatics, Comenius University, Mlynská dolina, 842 48 Bratislava, Slovakia.
Email: toth@fmph.uniba.sk
[2]CEMeNt – Central European Meteor Network
[3]PFN – Polish Fireball Network
[4]IMTN – Italian Meteor and TLE Network

IMO bibcode WGN-404-toth-draconids
NASA-ADS bibcode 2012JIMO...40..117T

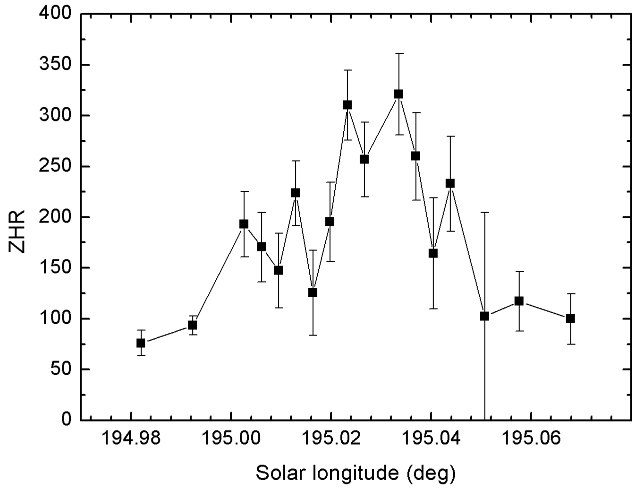

Figure 2 – Visual activity profile of the Draconids (2011 October 8–9) from the station Cavandola derived by J. Koukal.

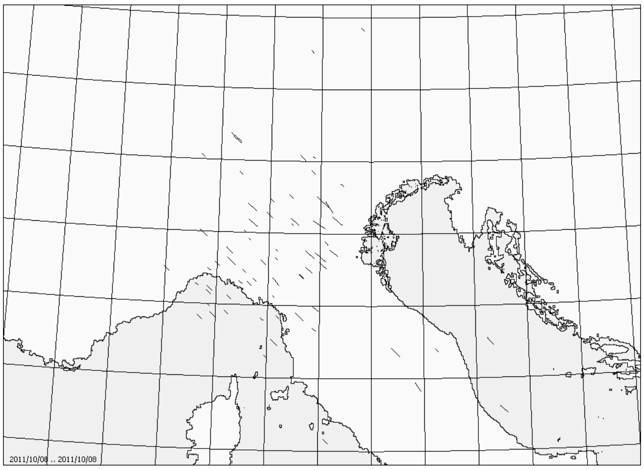

Figure 3 – Ground projection of the detected Draconid trails.

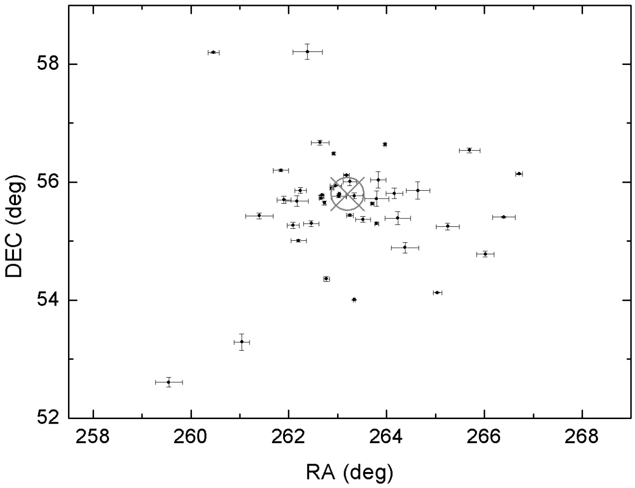

Figure 4 – Individual geocentric radiant positions (J2000.0) distribution of the Draconids in right ascension (RA) and declination (DEC). The expected radiant position $\alpha = 263\overset{\circ}{.}2$ and $\delta = 55\overset{\circ}{.}8$ according to Vaubaillon (2011a) is depicted as $\otimes$.

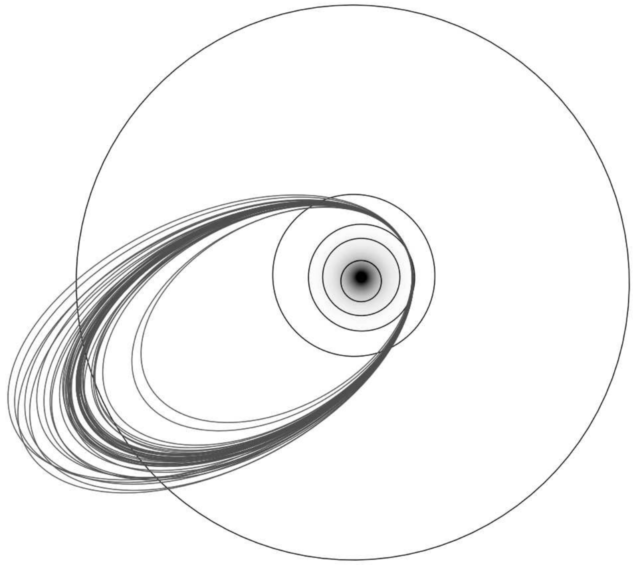

Figure 5 – Orbits of multi-station Draconids detected by video stations, derived by the UFOOrbit software. The orbits are projected onto the ecliptic plane. The orbits of Jupiter and the inner planets are also plotted. The direction to the vernal equinox is from the center to the right.

observations were performed during the maximum activity of the Draconids (2011 October 8–9), when 62 meteors were observed simultaneously at least from two stations.

During the observational interval the elevation of the Draconid radiant has changed from 68 to 29 degrees.

4 Results

The visual activity profile of the observed Draconids was derived according to IMO standards from the station Cavandola by J. Koukal (Figure 2). Observations were performed in 5 to 15 minutes intervals from $18^{\rm h}45^{\rm m}$ to $21^{\rm h}05^{\rm m}$ UT. There appeared two peaks at $19^{\rm h}50^{\rm m}$–$19^{\rm h}55^{\rm m}$ UT and at $20^{\rm h}05^{\rm m}$–$20^{\rm h}10^{\rm m}$ UT with ZHR of about 310 and 320, respectively. The mean population index of the Draconids was calculated as 2.62 ± 0.27 from the visual magnitude distribution in the interval -2 to $+5.5$ magnitude.

As was mentioned above, 62 meteors were identified as Draconids, simultaneously observed by video techniques in the time interval from $17^{\rm h}56^{\rm m}$ to $23^{\rm h}22^{\rm m}$ UT on October 8. The ground projection of the individual meteor trails as seen by the multi-station observation is depicted in Figure 3. After the precise reduction and inspection, 43 Draconids with sufficient precision were selected. An additional 19 possible Draconids were excluded due to small convergence angle of planes, small number of measured meteor positions or other geometrical and astrometrical issues which led to large trajectory uncertainty.

The orbit precision depends mostly on the accuracy of the velocity determination. Due to fragmentation of the Draconid meteoroids in the atmosphere and following deceleration, the measurement of meteor velocities was problematic and could be determined with large uncertainties. Therefore, according to Borovička et al. (2007) and Koten et al. (2007) we assumed the initial velocity of the Draconids as $23.57~\mathrm{km\,s^{-1}}$. This value was obtained from very precise photographic measurement of the Draconid fireball EN081005B in 2005 (Koten et al., 2007). The relevance of the assumption is supported by velocity fitting in several cases, where we were able to

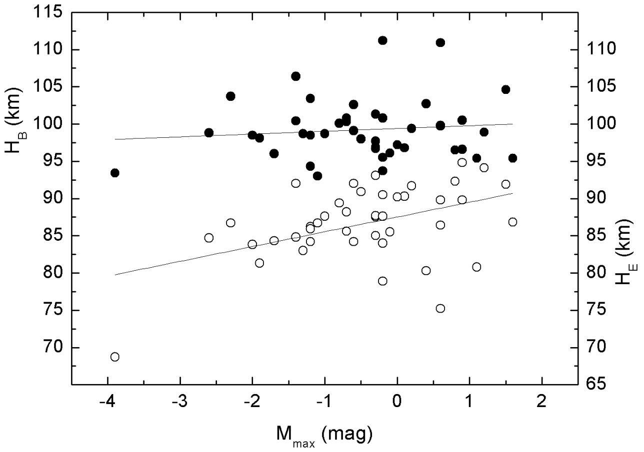

Figure 6 – The beginning (black circles) and terminal heights (open circles) of Draconids as a function of the absolute maximum brightness.

determine the deceleration in our video data. The geophysical data (geocentric radiant and velocity, absolute maximum brightness, beginning and terminal height) of 43 Draconids are listed in Table 1 and the orbital parameters are shown in Table 2 also with their standard deviations. The absolute brightness was determined with a lower precision of about ±1 magnitude and an error in the height of ±0.2 km. In Table 2, there is also presented the orbit of the parent comet 21P/Giacobini-Zinner obtained by a numerical integration from the epoch of comet's perihelion passage in 1900 to Oct., 2011. Individual geocentric radiant equatorial coordinates are shown in Figure 4. The mean radiant is $\alpha = 263.^\circ25 \pm 1.^\circ47$, $\delta = 55.^\circ61 \pm 1.^\circ00$. This is in good agreement with the expected radiant $\alpha = 263.^\circ2 \pm 0.^\circ2$ and $\delta = 55.^\circ8 \pm 0.^\circ2$ according to the model of Vaubaillon (2011a).

The heliocentric orbits projected on to the ecliptic plane are shown in Figure 5.

The beginning and endpoint heights as a function of the absolute maximum brightness of the Draconids are presented in Figure 6 and in the equation (1)

$$\begin{aligned} H_\mathrm{B} &= 99.4(\pm 0.7) + 0.4(\pm 0.5)\ M_\mathrm{max} \\ H_\mathrm{E} &= 87.5(\pm 0.8) + 2.0(\pm 0.6)\ M_\mathrm{max}, \end{aligned} \quad (1)$$

where H_B stands for the beginning height (km), H_E for the endpoint height (km) and M_max for the absolute maximum brightness (mag). However, the beginning heights do not change too much, which is a surprising result and will need detailed inspection. Naturally, the endpoint heights decrease with increasing brightness, which is standard for meteor showers.

5 Conclusion

We present geophysical data and heliocentric orbits of 43 Draconids obtained from multi-station video observations by the cameras of the Slovak Video Meteor Network (SVMN), the Central European Meteor Network (CEMeNt), the Polish Fireball Network and local Italian Meteor and TLE Network employed in Italy during the expected enhanced display of the Draconids on 2011 October 8. Comparison of the meteor shower orbits with the proposed parent body comet 21P/Giacobini-Zinner (JPL NASA) indicates a very close similarity. This work is a nice example of new video observations and cooperation of the networks in Poland, Czech Republic, Slovak Republic and Italy, which monitor regular and exceptional meteor activity as in the case of the Draconids 2011.

Acknowledgment This work was supported by the VEGA grant No. 1/0636/09, APVV-0516-10 grant and grant of Jozef Klačka. We greatly appreciate the help of Peter Vereš and video observations and data analysis done by professional and amateur astronomers of the video meteor networks and broad international cooperation and smooth data sharing.

References

Borovička J., Spurný P., and Koten P. (2007). "Atmospheric deceleration and light curves of Draconid meteors and implication for the structure of cometary dust". *Astron. Astrophys.*, **473**, 661–672.

Koten P., Borovička J., Spurný P., and Štork R. (2007). "Optical observation of enhanced activity of the 2005 Draconid meteor shower". *Astron. Astrophys.*, **466**, 729–735.

Molau S. (1999). "1983 TB and the Geminid Meteors". In Baggaley W. J. and Porubčan V., editors, *Proc. of the Meteoroids 1998 Conf.*, page 131, Bratislava.

SonotaCo (2009). "Ongoing meteor work. A meteor shower catalog based on video observations in 2007–2008". *WGN, Journal of the IMO*, **37:2**, 55–62.

Tóth J., Kornoš L., Gajdoš v., Kalmančok D., Zigo P., Világi J., and Hajdukov'a M. (2008). "TV Meteor Observations from Modra". *Earth, Moon, and Planets*, **102**, 257–261.

Tóth J., Kornoš L., Vereš P., Šilha J., Kalmančok D., Zigo P., and Világi J. (2011a). "All-Sky Video Orbits of Lyrids 2009". *Publ. Astron. Soc. Japan*, **63**, 331–334.

Tóth J., Vereš P., Kornoš L., Piffl R., Koukal J., Gajdoš v., Majchrovič I., Zigo P., Zima M., Világi J., and Kalmančok D. (2011b). "Video observation of Geminids 2010 and Quadrantids 2011 by SVMN and CEMeNt". *WGN, Journal of the IMO*, **39:2**, 34–38.

Vaubaillon J. (2011). "The 2011 Draconids meteor shower". IMC 2011 Sibiu, Romania, presentation.

Vaubaillon J., Watanabe J., Sato M., Horii S., and Koten P. (2011). "The comming 2011 Draconids meteor shower". *WGN, Journal of the IMO*, **39:3**, 59–63.

Watanabe J. and Sato M. (2008). "Activities of parent comets and related meteor showers". *Earth, Moon, and Planets*, **102**, 111–116.

Handling Editor: Javor Kac
This paper has been typeset from a LaTeX file prepared by the author.

Table 1 – Double and multi-station Draconids detected on 2011 October 8 by joint ground based video expedition in Italy. Individual geocentric radiants α_G, δ_G (J2000.0), V_g – geocentric velocity (computed with the assumed $v_\infty = 23.57$ km s^{-1}), M_{max} – absolute maximum brightness, H_B – beginning and H_E – endpoint height of meteors as well as acronyms of observing cameras are presented. Cameras: Bettola – all sky (BA), Bettola – north (BN), Bettola – south (BS), Cavandola – south (CS), Cavandola – north (CN), Nogara (Pa), Cuneo Ass. Astrofili Bisalta (CU), Ferrara south (FEs), Ferrara north-west (FEn), Fanano (FA), Fanano zenith (FAz), Contigliano – Rieti (TUs3), Teramo north (TUn), Teramo west (TUw). The mean geocentric radiant, the mean geocentric velocity, the mean beginning and terminal height in the observing time interval ($17^h55^m50^s$–$23^h21^m53^s$ UT) are also presented.

No	Time [UT]	α_G [°]	δ_G [°]	V_g [km s^{-1}]	M_{max} [mag]	H_B [km]	H_E [km]	Camera
1	17:55:50	263.80 ± 0.04	55.30 ± 0.02	20.85 ± 0.32	−1.2	103.4	86.2	BA-FEs
2	17:56:04	260.46 ± 0.11	58.20 ± 0.01	20.86 ± 0.76	−0.1	96.1	85.5	BA-CS
3	18:14:50	262.64 ± 0.18	56.67 ± 0.04	20.88 ± 1.09	−1.7	96.0	84.3	TUs3-FEs
4	18:28:11	263.18 ± 0.06	56.12 ± 0.01	20.88 ± 0.36	+1.1	95.4	80.8	CS-FAz
5	18:39:34	266.40 ± 0.23	55.41 ± 0.01	20.88 ± 1.41	+0.8	96.5	92.3	BA-CS
6	18:42:54	265.04 ± 0.09	54.13 ± 0.01	20.89 ± 0.53	−0.3	97.7	87.5	BA-CS
7	19:04:44	261.40 ± 0.28	55.43 ± 0.05	20.91 ± 1.39	+0.6	110.9	75.2	Pa-CN
8	19:07:16	263.34 ± 0.02	54.01 ± 0.01	20.91 ± 0.15	−1.1	93.0	86.7	BA-CN
9	19:07:32	262.96 ± 0.12	55.94 ± 0.01	20.90 ± 0.63	−0.3	96.7	85.0	BA-CN
10	19:11:26	259.55 ± 0.28	52.61 ± 0.08	20.93 ± 1.29	−0.2	111.2	78.9	Pa-CN
11	19:22:14	265.70 ± 0.21	56.54 ± 0.04	20.90 ± 1.13	+0.4	102.7	80.3	FA-Pa-BS
12	19:22:30	262.20 ± 0.16	55.01 ± 0.02	20.92 ± 0.68	−0.3	96.9	87.7	BA-CU
13	19:23:20	261.84 ± 0.16	56.20 ± 0.02	20.91 ± 0.73	+0.6	99.8	89.8	BA-CS
14	19:39:35	263.34 ± 0.17	55.77 ± 0.05	20.92 ± 0.86	−0.3	101.3	93.1	BS-CS
15	19:49:06	263.02 ± 0.16	55.76 ± 0.02	20.92 ± 0.63	−1.0	98.7	87.6	BA-CS-CU
16	19:58:45	263.52 ± 0.15	55.37 ± 0.05	20.93 ± 0.66	−3.9	93.4	68.7	BA-FEn-CN-BN
17	20:00:24	265.25 ± 0.24	55.25 ± 0.06	20.93 ± 1.04	+0.2	99.4	91.7	BA-CS
18	20:03:22	263.97 ± 0.02	56.64 ± 0.02	20.93 ± 0.10	−0.6	102.6	84.2	BA-FA
19	20:11:32	262.17 ± 0.23	55.68 ± 0.09	20.93 ± 1.05	+1.5	104.6	91.9	BA-CS
20	20:15:01	262.46 ± 0.16	55.30 ± 0.05	20.94 ± 0.68	+0.9	100.5	94.8	BA-CS
21	20:17:30	262.09 ± 0.12	55.27 ± 0.05	20.94 ± 0.47	−2.0	98.5	83.8	BA-TUs3-FEs-BN
22	20:18:27	266.71 ± 0.07	56.14 ± 0.01	20.93 ± 0.26	+1.2	98.9	94.1	BA-CS
23	20:20:07	262.66 ± 0.03	55.73 ± 0.02	20.93 ± 0.14	−1.2	98.5	85.9	BA-CN-BN
24	20:21:09	264.38 ± 0.28	54.89 ± 0.09	20.94 ± 1.17	+0.9	96.6	89.8	BA-CS
25	20:27:46	262.24 ± 0.12	55.86 ± 0.05	20.94 ± 0.58	+0.1	96.8	90.3	BA-CU
26	20:31:13	262.38 ± 0.30	58.21 ± 0.13	20.93 ± 1.29	−1.9	98.1	81.3	BA-CN-BN
27	20:31:40	263.03 ± 0.02	55.80 ± 0.01	20.94 ± 0.07	−0.7	100.3	88.2	BA-CS-CU
28	20:34:38	266.02 ± 0.18	54.78 ± 0.05	20.94 ± 0.66	−2.6	98.8	84.7	BA-CS-CU
29	20:37:03	262.88 ± 0.04	55.90 ± 0.02	20.95 ± 0.13	−2.3	103.7	86.7	TUs3-FEs
30	20:46:56	264.23 ± 0.26	55.39 ± 0.11	20.94 ± 1.06	+1.6	95.4	86.8	BA-CS
31	20:49:14	262.68 ± 0.03	55.78 ± 0.01	20.94 ± 0.01	−1.2	94.3	84.2	BA-CU
32	20:51:52	263.25 ± 0.07	55.44 ± 0.02	20.95 ± 0.16	−1.3	98.7	83.0	BA-CU
33	20:55:30	264.16 ± 0.17	55.81 ± 0.09	20.94 ± 0.74	−0.7	100.8	85.6	BA-CS
34	20:57:36	262.77 ± 0.06	54.36 ± 0.04	20.95 ± 0.25	−1.4	106.4	84.8	BA-CN
35	21:02:48	261.90 ± 0.14	55.70 ± 0.06	20.95 ± 0.47	−0.2	93.7	84.0	BA-CS-CU
36	21:04:05	263.25 ± 0.14	56.01 ± 0.07	20.95 ± 0.57	−0.6	99.1	92.0	BA-CN-BN
37	21:05:29	263.80 ± 0.25	55.72 ± 0.13	20.95 ± 1.06	+0.6	99.7	86.4	BA-CS
38	21:15:24	263.71 ± 0.03	55.64 ± 0.02	20.95 ± 0.16	−0.5	98.0	90.9	BA-CU
39	21:32:38	264.64 ± 0.24	55.86 ± 0.15	20.95 ± 1.04	0.0	97.2	90.2	BA-CS-CU
40	22:01:39	261.04 ± 0.16	53.29 ± 0.14	20.97 ± 0.66	−1.4	100.4	92.0	TUn-TUs3
41	22:22:08	263.83 ± 0.16	56.04 ± 0.14	20.95 ± 0.65	−0.2	100.8	90.5	BA-FAz
42	23:00:36	262.92 ± 0.02	56.49 ± 0.02	20.94 ± 0.03	−0.2	95.5	87.6	TUw-TUs3
43	23:21:53	262.73 ± 0.02	55.65 ± 0.03	20.93 ± 0.15	−0.8	100.1	89.4	BN-FEn
mean		263.25	55.61	20.93		99.2	86.6	
st. dev		1.47	1.00	0.03		4.0	5.1	

Table 2 – Double and multi-station Draconids detected on 2011 October 8 by joint ground based video expedition in Italy. The orbital elements (J2000.0) and observing cameras are presented. Cameras: Bettola – all sky (BA), Bettola – north (BN), Bettola – south (BS), Cavandola – south (CS), Cavandola – north (CN), Nogara (Pa), Cuneo Ass. Astrofili Bisalta (CU), Ferrara south (FEs), Ferrara north-west (FEn), Fanano (FA), Fanano zenith (FAz), Contigliano – Rieti (TUs3), Teramo north (TUn), Teramo west (TUw). The mean orbital elements (J2000.0) from the observing time interval ($17^h55^m50^s$–$23^h21^m53^s$ UT) are also presented. The Draconid fireball EN081005B from 2005 (Koten et al., 2007) is mentioned for comparison as well as the forward integrated orbit (JPL NASA) of the comet 21P/Giacobini-Zinner (1900) to the epoch Oct., 2011.

No	a [AU]	q [AU]	e	i [°]	ω [°]	Ω [°]	Camera
1	3.63 ± 0.25	0.9967 ± 0.0001	0.726 ± 0.019	31.49 ± 0.35	173.84 ± 0.05	194.9437	BA-FEs
2	2.80 ± 0.34	0.9956 ± 0.0001	0.645 ± 0.042	32.64 ± 0.86	172.33 ± 0.20	194.9439	BA-CS
3	3.22 ± 0.69	0.9964 ± 0.0001	0.691 ± 0.064	32.05 ± 1.20	173.41 ± 0.25	194.9568	TUs3-FEs
4	3.39 ± 0.25	0.9966 ± 0.0001	0.706 ± 0.021	31.83 ± 0.40	173.63 ± 0.08	194.9659	CS-FAz
5	3.80 ± 1.33	0.9979 ± 0.0001	0.737 ± 0.085	31.44 ± 1.52	175.69 ± 0.26	194.9737	BA-CS
6	4.16 ± 0.56	0.9971 ± 0.0001	0.760 ± 0.032	31.07 ± 0.56	174.39 ± 0.11	194.9760	BA-CS
7	3.47 ± 0.95	0.9952 ± 0.0001	0.713 ± 0.080	31.71 ± 1.55	172.15 ± 0.43	194.9910	Pa-CN
8	4.07 ± 0.14	0.9961 ± 0.0001	0.756 ± 0.009	31.12 ± 0.16	173.15 ± 0.03	194.9927	BA-CN
9	3.44 ± 0.44	0.9964 ± 0.0001	0.710 ± 0.037	31.81 ± 0.69	173.41 ± 0.17	194.9929	BA-CN
10	4.23 ± 1.55	0.9926 ± 0.0002	0.766 ± 0.078	30.83 ± 1.38	170.04 ± 0.43	194.9955	Pa-CN
11	3.44 ± 0.86	0.9979 ± 0.0001	0.710 ± 0.066	31.90 ± 1.25	175.52 ± 0.27	195.0029	FA-Pa-BS
12	3.65 ± 0.55	0.9956 ± 0.0001	0.728 ± 0.041	31.53 ± 0.74	172.61 ± 0.23	195.0031	BA-CU
13	3.31 ± 0.48	0.9958 ± 0.0001	0.699 ± 0.043	31.96 ± 0.81	172.69 ± 0.23	195.0037	BA-CS
14	3.51 ± 0.64	0.9965 ± 0.0001	0.716 ± 0.050	31.75 ± 0.95	173.63 ± 0.25	195.0148	BS-CS
15	3.50 ± 0.48	0.9964 ± 0.0001	0.716 ± 0.037	31.76 ± 0.69	173.40 ± 0.22	195.0213	BA-CS-CU
16	3.65 ± 0.51	0.9965 ± 0.0001	0.727 ± 0.038	31.62 ± 0.73	173.64 ± 0.21	195.0280	BA-FEn-CN-BN
17	3.81 ± 0.94	0.9974 ± 0.0001	0.738 ± 0.062	31.49 ± 1.13	174.83 ± 0.31	195.0291	BA-CS
18	3.33 ± 0.06	0.9971 ± 0.0001	0.701 ± 0.006	32.03 ± 0.12	174.33 ± 0.03	195.0311	BA-FA
19	3.47 ± 0.76	0.9958 ± 0.0002	0.713 ± 0.060	31.79 ± 1.17	172.77 ± 0.36	195.0367	BA-CS
20	3.60 ± 0.53	0.9959 ± 0.0001	0.724 ± 0.040	31.64 ± 0.75	172.87 ± 0.24	195.0391	BA-CS
21	3.59 ± 0.34	0.9956 ± 0.0001	0.722 ± 0.027	31.65 ± 0.52	172.59 ± 0.17	195.0408	BA-TUs3-FEs-BN
22	3.62 ± 0.20	0.9981 ± 0.0001	0.724 ± 0.015	31.74 ± 0.29	176.09 ± 0.08	195.0415	BA-CS
23	3.49 ± 0.10	0.9961 ± 0.0001	0.715 ± 0.008	31.79 ± 0.16	173.13 ± 0.04	195.0426	BA-CN-BN
24	3.87 ± 1.11	0.9969 ± 0.0002	0.743 ± 0.069	31.42 ± 1.28	174.11 ± 0.37	195.0433	BA-CS
25	3.43 ± 0.39	0.9959 ± 0.0001	0.710 ± 0.033	31.85 ± 0.65	172.87 ± 0.18	195.0479	BA-CU
26	2.91 ± 0.55	0.9967 ± 0.0002	0.657 ± 0.069	32.64 ± 1.52	173.69 ± 0.50	195.0502	BA-CN-BN
27	3.50 ± 0.05	0.9964 ± 0.0001	0.715 ± 0.004	31.80 ± 0.08	173.42 ± 0.03	195.0505	BA-CS-CU
28	4.04 ± 0.62	0.9976 ± 0.0001	0.753 ± 0.039	31.31 ± 0.72	175.23 ± 0.23	195.0526	BA-CS-CU
29	3.47 ± 0.10	0.9963 ± 0.0001	0.713 ± 0.008	31.85 ± 0.14	173.33 ± 0.05	195.0542	TUs3-FEs
30	3.70 ± 0.89	0.9969 ± 0.0002	0.731 ± 0.062	31.61 ± 1.17	174.15 ± 0.36	195.0610	BA-CS
31	3.49 ± 0.10	0.9961 ± 0.0001	0.714 ± 0.010	31.81 ± 0.10	173.16 ± 0.10	195.0626	BA-CU
32	3.62 ± 0.13	0.9964 ± 0.0001	0.725 ± 0.010	31.67 ± 0.18	173.47 ± 0.10	195.0644	BA-CU
33	3.57 ± 0.56	0.9970 ± 0.0001	0.721 ± 0.043	31.75 ± 0.83	174.21 ± 0.25	195.0669	BA-CS
34	3.94 ± 0.23	0.9957 ± 0.0001	0.747 ± 0.015	31.32 ± 0.28	172.82 ± 0.08	195.0683	BA-CN
35	3.46 ± 0.30	0.9956 ± 0.0001	0.712 ± 0.026	31.83 ± 0.51	172.58 ± 0.21	195.0719	BA-CS-CU
36	3.46 ± 0.42	0.9965 ± 0.0001	0.712 ± 0.033	31.87 ± 0.65	173.63 ± 0.20	195.0727	BA-CN-BN
37	3.58 ± 0.81	0.9968 ± 0.0002	0.721 ± 0.060	31.74 ± 1.19	173.93 ± 0.37	195.0737	BA-CS
38	3.60 ± 0.12	0.9967 ± 0.0001	0.723 ± 0.009	31.72 ± 0.18	173.84 ± 0.04	195.0805	BA-CU
39	3.59 ± 0.80	0.9972 ± 0.0002	0.723 ± 0.059	31.76 ± 1.18	174.55 ± 0.35	195.0923	BA-CS-CU
40	4.17 ± 0.68	0.9941 ± 0.0002	0.762 ± 0.038	31.04 ± 0.74	171.28 ± 0.26	195.1122	TUn-TUs3
41	3.49 ± 0.45	0.9968 ± 0.0001	0.714 ± 0.036	31.85 ± 0.76	174.03 ± 0.25	195.1262	BA-FAz
42	3.31 ± 0.10	0.9964 ± 0.0001	0.699 ± 0.010	32.04 ± 0.30	173.51 ± 0.30	195.1526	TUw-TUs3
43	3.51 ± 0.10	0.9961 ± 0.0001	0.717 ± 0.008	31.75 ± 0.18	173.12 ± 0.04	195.1672	BN-FEn
mean	3.58	0.9964	0.720	31.70	173.51		
st. dev	0.29	0.0010	0.023	0.34	1.10		
EN081005B	3.53	0.99606	0.717	31.74	173.25	195.51097	
st. dev	0.07	0.00010	0.005	0.10	0.12	0.00001	
21P	3.519	1.032	0.707	31.905	172.574	195.403	

Draconids expedition to the Adriatic

Krisztián Sárneczky[1] *and Antal Igaz*[2]

A personal account of the 2011 October 8 Draconid outburst observations is given.

Received 2012 February 5

1 Introduction

Our team kept an eye on the weather forecast the whole week and were ready to travel anywhere in a radius of 1000 km. The weather on the morning before the Draconids night did not look promising, so we nervously contacted all our friends in the region. Attila Gazdag gave a promising report from South-East Hungary and we knew that the Polish team had gone to Italy. Satellite images indicated a gap in the cloud covering above northern Italy. So, we headed towards the Adriatic and by 4 o'clock in the afternoon we were on the Hungarian border to Croatia. Finally Javor Kac gave us a tip, confirming that although it was raining at the moment, in two hours we can expect some clear skies over western Slovenia. We decided to join the Slovenian team on Slavnik Peak, close to the village of Podgorje. We saw a tiny clear stripe of blue sky on the horizon all the way to Ljubljana and as we drove further south the clouds started to disappear behind us. Time was running out, we only had an hour before the predicted outburst but we knew we would not make it in time to meet up with the Slovenian group. So, we just stopped at the best possible location on the side of a village road and quickly set up our mattresses, sleeping bags and cashier machine paper rolls.

2 Observations

During our preparation, we had already seen some nice, slow Draconids, further confirming that our journey was not in vain. We began our official observations exactly at 9 pm local time ($19^{h}00^{m}$ UT), with a 10–15% cloud cover. Based on the magnitude 4.3–4.7 comparison stars for the variable star g Herculis, the limiting magnitude was about 5.0, even with a very bright Moon. We arranged our fields of view to the West and to the North – right to the radiant – which was not ideal, but still the best option.

The meteors arrived in groups with 3–4 minutes breaks. We were just beginning to get worried when we saw our first real shower of the Draconids at $19^{h}59^{m}$ UT. There were six meteors in a row, one in every second. After a little break, there were some faint meteors that followed, some of them appeared within the same second, others arrived in a sequence with a few seconds difference. The brightest one was of magnitude 0, whereas most of them were in the range of magnitude +2 to +4. It became obvious for both of us that we were observing the maximum peak of the shower, almost exactly at the predicted time, maybe with a 5–10 minutes delay. The most spectacular event was a twin meteor, falling along close, parallel lines, 20 arc minutes from each other in Cepheus, with the same brightness and same length, the likes of which neither of us had seen before.

Terms we would use to describe the typical look of the meteors include short, faint, diffuse, for instance. They appeared as spitting objects, fuzzy, blurred, hazy and lacking any of the sharp and fast appearance that the Gemininds or Perseids display. We both often had the feeling there were some faint and hazy meteors, just below our own limiting magnitude, which we were, therefore, unable to positively identify and record. Our conclusion was that the Draconids have very special characteristics, unlike anything we have seen before.

We saw two meteors, which were quite faint, then disappeared, that then showed up again along their lines of trajectory, but in a notably brighter form. We are guessing that the missing section was simply fainter than our limit sensitivity, so it "disappeared" from our view. This explanation was later confirmed by Zsófia Biró's photo, taken in Budapest, Hungary. Again, this was something we have never seen before. Our conjecture is that it might be explained by its fresh comet origin, combined with a slow entering velocity.

Later, just as they arrived, the Draconids started to disappear. Starting from $20^{h}20^{m}$ UT, we observed only smaller groups, with longer breaks in between. At the same time, the average brightness of the meteors definitely increased on a slope; we recorded meteors with magnitudes of 0, −1, −2. The most spectacular one was a magnitude −3 Draconid on the border of Cepheus with a persistent train lasting for a few seconds. It seems that the larger particles had gradually drifted to the edge of the cloud. At $21^{h}00^{m}$ UT we had the feeling that we have seen the highlight of the shower's outburst and we could start on our way back home. We kept observing for another 15 minutes, having only seen a few meteors, interdispersed between 5-minute breaks, when new cloud coverage began to advance from the North. Combined we recorded 98 Draconids and 8 sporadic meteors in 4.26 hours and were very happy that we did not miss this spectacular event. It was also extraordinary to witness the accuracy of this prediction.

Handling Editor: Javor Kac

[1]Göncöl u. 43., XIV/II/11, H-1131 Budapest, Hungary. Email: sky@titan.physx.u-szeged.hu

[2]Húr u. 9/D, H-1223 Budapest, Hungary. Email: antaligaz@yahoo.com

IMO bibcode WGN-404-sarneczky-draconids
NASA-ADS bibcode 2012JIMO...40..122S

The Dragon spitting fire all over the starry sky in Portugal

Michel Vandeputte [1]

The Draconid meteor outburst was successfully observed from Vendinha, Portugal. Visual observations with high resolution data (1 minute intervals) detected a maximum peak around solar longitude $195\overset{\circ}{.}03 - 195\overset{\circ}{.}04$ ($\lambda_{\odot}$ 2000.0) with ZHR 368 ± 87 corresponding to 2011 October 8, $\sim 20^{\mathrm{h}}15^{\mathrm{m}} \pm 5^{\mathrm{m}}$ UT. This article describes my personal impression as visual observer during a last minute Draconid expedition to Portugal.

Received 2012 April 19

1 Introduction

On October 6 I did not have any plans to observe the Draconids. I was very busy doing other work and I hadn't asked for any free days for this event because the Draconid outburst would occur during the weekend. Almost all my friends had already gone on expedition or made plans to watch the outburst while I hadn't made any plans. But on that special evening of October 6, I definitely changed my mind and focused on the Draconids. I read different articles and reviewed all the predictions for the shower (Vaubaillon et al., 2011; Maslov, 2011). I concluded that this was very likely a 'not to be missed event', moreover this could be for me, as a dedicated meteor observer, a once in a lifetime experience with a very rare Draconid meteor outburst. Despite the interfering moon here in Western Europe we were located in the front row for this special event with the radiant high in the evening sky at the time of maximum activity. It was time to take the initiative and act!

2 The preparation

First I had to make the most important decision: where to go? My own country, Belgium, was definitely excluded because of the arrival of a warm front including cloud cover and some rain showers during October 8–9. I analysed the latest weather forecasts for the weekend and I found two suitable sites on the West European weather charts.

The first possibility was to travel towards the North-East and join a group of DMS observers located in northern Germany. Danish Jutland and some parts of northern Germany enjoy some protection from the weather by Norwegian mountains that offer a great chance to find a large area of clear skies between two bad weather systems. The problem with this plan was that we had to travel too many kilometres by car in too little time and there was also some risk with the local weather (high humidity, fog, etc.).

The second possibility was to go to the Iberian peninsula (Spain and Portugal). These countries are influenced by the Azores high pressure system which produces with almost 100% certainty clear and dry skies. I had some advantages for this location as I had travelled twice to Portugal with DMS to observe the Geminids in 2007 and 2009 and I know of some observing sites in the dark outback of Portugal (Miskotte et al., 2011). Another advantage was that the lower humidity would reduce the negative effects from the interfering moonlight during the peak activity as it was predicted that the main outburst around 20^{h} UT consisted mostly of faint meteors. I decided not to take any further risks and choose the 'safe' Portugal plan.

I checked the astronomical conditions for my observing place in Portugal with planetarium software and I found some disadvantages for the location. At 20^{h} UT, the moon would be located 6° higher in the sky than in Belgium. Observations of the possible maximum from the older dust trails around 17^{h} UT would be impossible. The observing window in darkness before the predicted peak was very short with only one hour of effective observing before the time of the maximum activity. This could become tricky in case the outburst occurred sooner than expected. The radiant altitude at peak time (56° at 20^{h} UT), was as high as in Belgium and was no problem. The conclusion was that Portugal wasn't the best place to observe the Draconids but I was assured to have a clear sky that night.

The first step of my last minute expedition was done; I found the location. The next challenge of that evening was to book a flight from Brussels to Lisbon for me and my girlfriend with a suitable time schedule for our last minute Draconid expedition. This proved to be rather difficult as only a few seats were left but I succeeded. I found a flight from Brussels to Lisbon with departure in the early morning of Saturday, October 8 and a return on Sunday, October 9 around 10^{h} a.m. By midnight the whole schedule of our mini Draconid expedition was ready for take off on Saturday, October 8!

3 The journey

My girlfriend and I left very early in the morning and enjoyed a relaxing flight above a mostly clouded France and Gulf of Biscay. All the clouds were gone once over the Picos d'Europe (a mountain chain in Northern Iberia). Weather conditions were great in Lisbon, Portugal. It was sunny with temperatures of over 20°C with only a few patches of cirrus clouds. We hired a car and travelled about 140 kilometers in an eastern direction to our destination: Évora. This town is the capital of the province Alentejo where we stayed for most of the day. Évora is a UNESCO world heritage site. The old town center is partially enclosed by medieval walls and there are many historical monuments such as a Roman temple, buildings influenced by the occupation by the

[1]Cachette Pierrette 78, 9600 Ronse, Belgium
Email: michelvandeputte@hotmail.com

IMO bibcode WGN-404-vandeputte-draconids
NASA-ADS bibcode 2012JIMO...40..123V

Moors and many ancient churches. In the late afternoon we left the city and travelled for another 30 kilometers in an eastern direction to our observing place. We choose the site that we used for the 2007 Geminid return, situated nearby a small village called Vendinha.

We enjoyed our dinner and waited for the sunset at the edge of a local lake near our observing site. The nearly full moon was rising in the east while the last cirrus clouds disappeared. The final preparations were made; checking all the equipment, the limited magnitude counting areas, calibrating my time clocks with interval alarms, etc. Around 18^{h} UT we arrived at our observing place. The sunset was beautiful and a bright colourful Venus Belt over the east introduced a clear night over Portugal. With the enjoyable air temperature of 20°C, the crickets were making lots of noise. I thought that this was the beginning of a normal Perseid watch somewhere in the French Provence but it wasn't; this time we were waiting for the Draconids!

4 The Draconid outburst

At $18^{\mathrm{h}}45^{\mathrm{m}}$ UT everything was ready. I was watching the northern sky but with the twilight it wasn't dark yet. Big owls were flying low over our heads and a giant Eagle-owl was exploring our car; I hoped he wouldn't find or damage the screen wipers. The first stars appeared and I was searching for all known constellations in that area of the sky. Suddenly I saw my first meteor; a slow one with a short trail somewhere in the northern direction. Shortly after the first one; a second – look-alike – meteor appeared into the direction of Polaris. Both meteors came from the head of Draco, so for sure, these had to be Draconids! In that first 'official' period while the twilight faded I counted 4 Draconids. That was more than during my 20 year career as meteor observer!

I decided to start my official meteor session at 19^{h} UT. I counted 7 Draconids in the first period of 10 minutes and my personal visual limited magnitude reached 6.0. The meteor activity got progressively stronger. I decided to start using 'one minute interval counting' in case the activity greatly increased during the session, something that I learned from the Leonid meteor storms. Most meteors were faint and often showed a short trail. I was absolutely fascinated by the irregular light profiles of the Draconids. This told us something about how fragile these meteors were. In the literature Draconids are described as very slow meteors; but personally I did find them rather fast. Nevertheless, this shower is unique to witness and you can't compare it with any other meteor shower.

The Draconid activity increased after $19^{\mathrm{h}}20^{\mathrm{m}}$ UT. Minute counts with 2–3 meteors became frequent. Most meteors were faint. What would this have been without the interfering moonlight? I saw another increase in activity around $19^{\mathrm{h}}40^{\mathrm{m}}$ UT when my minute counts topped 4 Draconids. At $19^{\mathrm{h}}50^{\mathrm{m}}$ UT I counted 5 meteors! At some moments I observed two Draconids at once! The activity was strong and the peak activity was obvious when we reached the predicted time of maximum activity published by Jeremie Vaubaillon et al. (2011). Very shortly after 20^{h} UT a sudden dead period in the shower activity occurred which lasted some minutes. I thought the show was over.

Fortunately this wasn't the case and meteor activity picked up again with another series of strong minute counts; 5 Draconids at $20^{\mathrm{h}}10^{\mathrm{m}}$ and $20^{\mathrm{h}}14^{\mathrm{m}}$ UT, 7 Draconids at $20^{\mathrm{h}}15^{\mathrm{m}}$ UT! I was thrilled! The Draconids became a bit brighter and showed many more long paths over the Portuguese moonlit night sky. Also the first Draconids with negative magnitudes showed up. At $20^{\mathrm{h}}21^{\mathrm{m}}$ UT I observed an awesome burst of three Draconids at the same moment! Besides the fact than the interfering moonlight became brighter and the Draconid radiant was getting lower; meteor activity stayed enjoyable high with lots of minute counts of 4 Draconids. It was an amazing show! I was wondering how long this outburst would last at this level?

I got the answer soon when someone pushed the red button at $20^{\mathrm{h}}30^{\mathrm{m}}$ UT. The Draconid activity decreased suddenly and dramatically. After another dead moment in activity; the shower recovered a bit and remained at an activity level of a regular two Draconids per minute. At $20^{\mathrm{h}}45^{\mathrm{m}}$ UT I observed my brightest Draconid of the night: a yellow -2 Draconid in Cepheus. After 21^{h} UT the minute counts without one single Draconid got the upper hand. Draconids became rare meteors and the outburst was definitely over. The broad and lower background activity took over and produced some final Draconid meteors. I saw only four Draconid meteors during my last half hour of observing. I was getting tired and I finally stopped the session at 22^{h} UT. The moonlight became too strong to continue observing and the Draconids were gone. A single bright Taurid took over the show.

Overall I was very happy with the result of this remarkable meteor observing session. During this evening session of three hours I logged 267 meteors including 250 Draconids. Hourly Draconid counts between 19^{h}–22^{h} UT were: 105 – 122 – 23 Draconids (or 154 Draconids between $19^{\mathrm{h}}30^{\mathrm{m}}$ and $20^{\mathrm{h}}30^{\mathrm{m}}$ UT). I was surprised how fast the Earth crossed through a dust trail of comet Giacobinni-Zinner and it was wonderful that these predictions were successfully made by Vaubaillon et al. (2011).

I closed my eyes and woke up again around 3^{h} UT. It was cold, the moon was nearly set. The night sky was filled with all the famous winter constellations and without the moon; the Portuguese sky became gorgeous and dark again. This was the same sky we enjoyed for the great Geminid return in 2007. We left our observing place and returned to Lisbon where we took our flight back to rainy Brussels. It was definitely worth spending some time for this great event. We saw the Dragon spitting fire all over the starry night.

5 Data analyses

The ZHR profile is shown in Figure 1 and is based on 10 minute interval periods. The ZHR was calculated assuming a population index of $r = 3.3$ based on the mag-

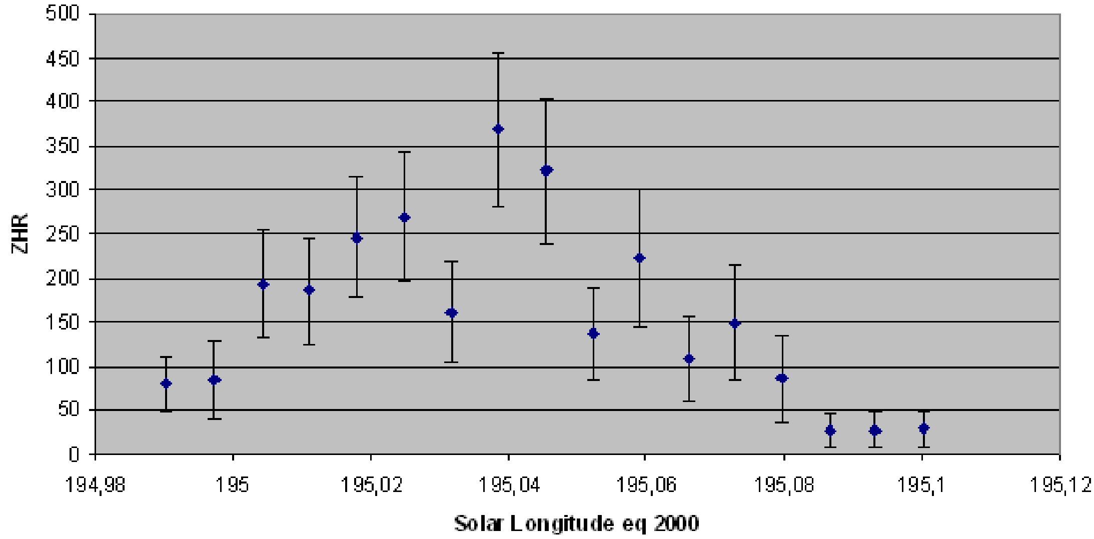

Figure 1 – ZHR profile based on 10 minute intervals for the Draconids 2011 by VANMC.

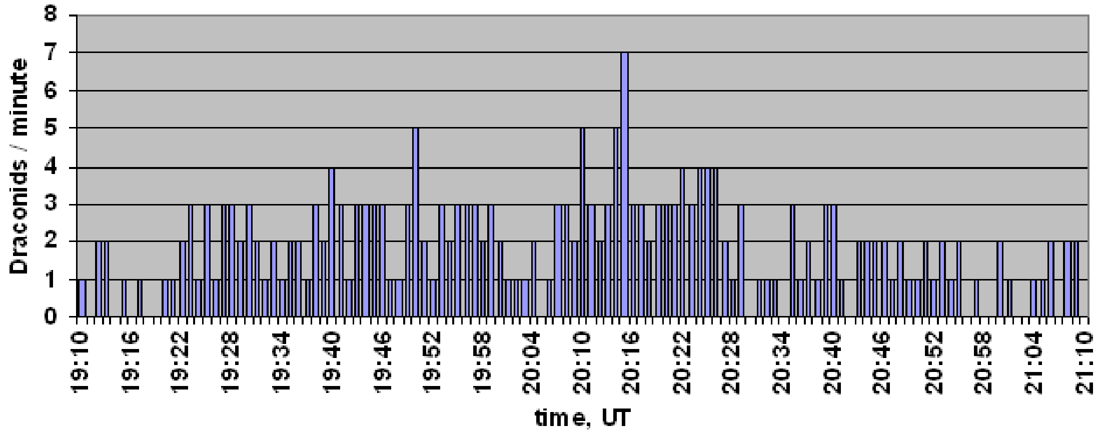

Figure 2 – Draconids 1 minute counts (VANMC).

nitude distribution of this data set. A personal perception coefficient C_p of 1.3 was taken into consideration as calculated for VANMC (Johannink et al., 2008). The highest ZHR occurred around solar longitude 195.°03 – 195.°04 ($\lambda_\odot$ 2000.0) with a ZHR 368 ± 87 corresponding to 2011 October 8, ~ $20^h15^m \pm 5^m$ UT. Figure 2 presents the one minute counts between 19^h10^m and 21^h10^m UT.

6 Acknowledgement

I would like to thank my girlfriend Inneke Vanderkerken for the big support, Carl Johannink and Koen Miskotte for analysing the meteor data. Also a word of thanks to Paul Roggemans for reviewing and translating the article.

References

Johannink C., Miskotte K., Jobse K., Vandeputte M., and van Leuteren P. (2008). "Results of the Aquariid expedition to La Palma, July 2008". *WGN, Journal of the IMO*, **36:6**, 139–146.

Maslov M. (2011). "Future Draconid outbursts (2011–2100)". *WGN, Journal of the IMO*, **39:3**, 64–67.

Miskotte K., Johannink C., Vandeputte M., and Bus P. (2011). "Geminids: 30 years of observations (1980–2009)". *WGN, Journal of the IMO*, **39:6**, 167–186.

Vaubaillon J., Watanabe J., Sato M., Horii S., and Koten P. (2011). "The coming 2011 Draconids meteor shower". *WGN, Journal of the IMO*, **39:3**, 59–63.

Handling Editor: Paul Roggemans
This paper has been typeset from a LaTeX file prepared by the author.

SPA Meteor Section Results: Radio Draconids 2011

Alastair McBeath[1]

Information determined from an analysis by the SPA Meteor Section of radio meteor data collected during the 2011 Draconid epoch is presented and discussed. A strong single maximum for the shower was found on October 8, with a mean time of $20^h05^m \pm 5^m$ UT, and that activity was above half the maximum flux level between $\sim 19^h20^m$ to 20^h45^m UT. A comparison is given too with the IMO's preliminary visual and video findings, which suggested a quite close correlation between all three observing techniques in what was detected. A possibility that more somewhat larger particles/brighter meteors may have been present between $\sim 19^h40^m$ to 20^h20^m UT is noted too.

Received 2012 June 9

1 Introduction

Despite being significantly affected by bright moonlight, the 2011 Draconid epoch was eagerly awaited by observers, with a number of possibly strong maxima predicted in advance to occur at sometime between roughly 16^h and 21^h UT on October 8–9 (see for example the two papers in the 2011 June *WGN*, **39:3**, pp. 59–67 (Vaubaillon et al., 2011; Maslov, 2011)). These predictions also proposed that activity relatively earlier in the 16^h–21^h interval (albeit dependent on just when the first stronger activity began within it) might be composed of somewhat larger dust particles, perhaps able to produce brighter meteors, and that conversely, activity relatively later in this spell might be of somewhat smaller particles/fainter meteors, which latter might prove undetectable visually in the moonlit sky.

Unfortunately, SPA British observers were largely clouded-out on the key night, with the exception of those at a few places in southern England and on the Channel Islands, although even they often saw far less than they might have hoped. Elsewhere in mainland Europe, conditions were thankfully often much better, allowing an excellent record of what took place to be made both visually and by video, as already presented in IMO reports (visually via the "live" online preliminary results at `www.imonet.org/draconids`; by video see Molau et al., 2012).

These IMO analyses largely concurred in finding a single Draconid maximum, with an estimated visual ZHR of ~ 300, at $20^h11^m \pm 1^m$ UT on October 8, and a FWHM from *circa* 19^h20^m to 20^h40^m UT. Visual and video reports received by the SPA Meteor Section, being far fewer in number, naturally could add nothing significant to these findings, but a detailed analysis of the radio results collected by the Section was possible, and it is primarily that which is presented here.

2 The Observers

The full list of contributing observers follows, including reports sent in directly, posted on the Draconids topics of the SPA and UK Weather World's Space Weather Forums (homepages at `www.popastro.com` and `www.ukweatherworld.co.uk` respectively), or kindly forwarded from the Arbeitskreis Meteore via their journal *Meteoros* **14:12** for 2011 December, provided by Ina Rendtel (see `www.meteoros.de`), from the North American Meteor Network by Rich Taibi (see web page `www.namnmeteors.org`), from 2011 November's *The Astronomer* magazine, courtesy of Tony Markham (see `www.theastronomer.org`) and from Radio Meteor Observation Bulletin 219 for 2011 October by Chris Steyaert (see `www.rmob.org`). In the list, "R" means radio observations were provided, "Vi" video or other imaging and "V" visual. Where not stated, purely visual data were received.

Chris Alder (England), Enric Algeciras (Spain; R), Rainer Arlt (Germany), Stela Arlt (Germany), Orlando Benitez (Canary Islands; R), Mike Boschat (Nova Scotia, Canada; R), Jens Briesemeister (Germany), Jeff Brower (British Columbia, Canada; R), Willy Camps (Belgium; R), Gaspard De Wilde (Belgium; R), Paul Domaille (Channel Islands), Franky Dubois (Belgium; R), David Entwistle (England; R), Frank Enzlein (Germany), Mike Feist (England), Richard Fleet (England), Karl-Heinz Gansel (Germany; R), Luc Gobin (Belgium; R), Mathias Growe (Germany), Shy Halatzi et al. (Israel), Oliver Hanke (Germany), Colin Henshaw (Saudi Arabia), "Jane B" (England), Peter Knol (Netherlands; R), Martin Krüge (Germany), Marco Langbroek (Germany; Vi & V), Hartwig Lüthen (Germany), Pierre Martin (Ontario, Canada), Paul Martsching (Iowa, USA), Michael McNeill (England), Sirko Molau (Germany), Mike Otte (Illinois, USA; R), Jürgen Rendtel (Germany), Steve Roush (Arizona, USA; R), Wayne Sanders (British Columbia, Canada; R), Mikiya Sato (Uzbekistan), Christian Schmiel (Germany), Stefan Schmeissner (Germany), Kai Schultze (Germany), Andy Smith (England; R), Ulrich Sperberg (Germany), Chris Steyaert (Belgium; R), Enrico Stomeo (Italy; Vi), Mikhail Svoiski (Arizona, USA; R), Istvan Tepliczky (Hungary; R), Felix Verbelen (Belgium; R), A O Woost (Germany).

3 Radio analysis method

As regular readers of this journal will know, the method I have developed for radio meteor analyses since the mid 1990s involves comparing the raw hourly radio meteor counts reported per system from day to day with one another during the interval a given shower's radiant could be observed for each radio receiver's location, al-

[1] 12a Prior's Walk, Morpeth, Northumberland, NE61 2RF, England, UK. Email: `spameteors@popastro.com`

IMO bibcode WGN-404-mcbeath-draconids
NASA-ADS bibcode 2012JIMO...40..126M

lowing for the daily variation in sporadic rates and any identifiable interference. These individual results are then compared between systems, looking for confirmation and correlation of what each detected separately, and between the main geographic regions the observers were located, usually Europe and North America.

It has often been difficult to know how best to present these results in a meaningful way in papers such as this, with the previously preferred method having been to give a few representative raw radio graphs with appropriate additions, such as radiant elevation curves. These have never been wholly satisfactory, so I changed this in late 2010 to hopefully give a more useful representation of what was found.

During my normal radio analyses, I have long assigned simple numerical values to indicate times when probable shower activity significantly different to normal was detected by a given observer's system. "Normal" here means periods when few or no shower meteors should have been present, as well as periods when shower meteors were detected at a lower level around the same time on nearby days. Zero indicates the normal state, and a positive number shows increased or otherwise unusual activity.

Combining this individual-system numerical information (sometimes with an element of weighting to allow for variable factors, such as a large number of active observers in one region but not another) allows a single total to be allocated to a particular time interval, based on what activity was detected, by how many different systems and where they were located. We can call this combined number the "Relative Radio Rate" (RRR). With care, often this can reveal the approximate timing of a given shower's maximum, as well suggesting how shower rates may have evolved near then.

It is important to appreciate the RRR is not a strictly-computed value, because there is a degree of subjectivity involved in assigning numbers to specific intervals per system. It is thus **not** the radio equivalent to the visual ZHR. However, by normalizing the assigned values to the ZHR, or plotting out the RRR using the second y-axis, it becomes practical to directly compare the patterns of activity detected visually and by radio, although not their absolute values. This approach has been presented here graphically for the first time in print.

4 2011 Draconid radio results

Figure 1 shows a plot of the RRR for the 24h period between 04^h00^m on October 8 to the same time on October 9, drawing on most of the viable radio meteor information, as observers typically provided results in the usual hour-long data bins only. The IMO visual ZHRs which were given numerically online from this interval are plotted too for comparison, but have here been combined into single hourly datapoints without error-bars for clarity. This suggested probable radio Draconid activity had been present from about 14^h UT on October 8 until $\sim 02^h$ on October 9, at least at a level liable to be readily detected visually or by video,

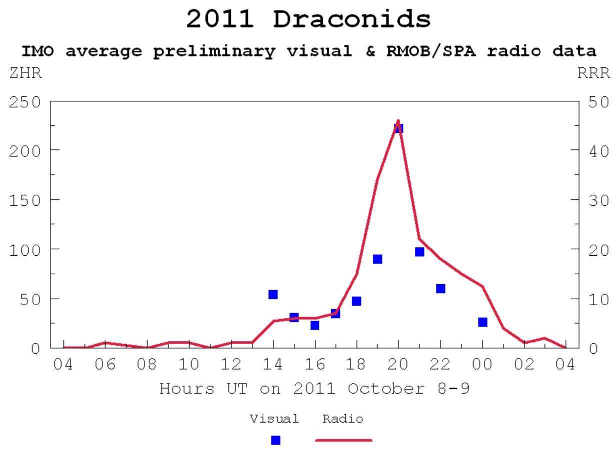

Figure 1 – A comparison of the Draconid RRR with the ZHR on October 8–9.

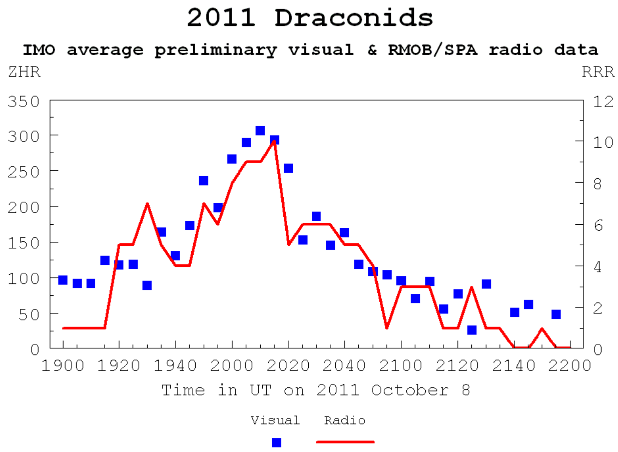

Figure 2 – A comparison of the radio and visual shorter time-interval Draconid data on October 8, averaged into five-minute bins.

with a distinct peak signature in the hour beginning at 20^h00^m UT. The pattern was quite closely comparable to that found in the IMO visual results (albeit with at least hourly datapoints available only between 14^h30^m to 23^h55^m UT on October 8). The IMO video information was generally comparable to the visual results on this timescale at the resolution of the graphs in (Molau et al., 2012), although with most of the observers based in Europe, the video activity graph ran near-continuously from just 17^h10^m to 23^h35^m UT). The radio findings also confirmed that despite the various predicted maximum timings for the UT evening hours, only one clear peak had actually occurred.

Jeff Brower, Gaspard De Wilde, Chris Steyaert and Mikhail Svoiski additionally provided counts of meteor echoes in shorter periods across the Draconid peak, the bins here lasting between 5 to 10 minutes. These allowed a more detailed examination of activity in the hours around the maximum, presented in Figure 2. A direct comparison between the IMO's visual and the these radio results showed again a closely similar pattern, with seemingly even many of the minor fluctuations between individual datapoints found in both sets. The radio information also found activity at or above half the maximum flux had been present from 19^h20^m

to 20^h45^m UT or so, virtually identical to what the video results found for the FWHM time. The mean UT time for the radio peak was $20^h05^m \pm 5^m$. These were naturally very pleasing findings, allowing further confirmation of what the earlier visual and video analyses had indicated.

While recalling the caveats regarding the analysed radio findings, there could be a suggestion in Figure 1 that between roughly 18^h and 01^h UT on October 8–9, excepting the hour including the shower's peak, there was a slightly higher level of radio Draconid activity overall than that found visually and by video. In turn this might suggest that a proportion of meteors too faint to be recorded except by radio were present at such times. Unfortunately, of the four observers who provided shorter time-bin echo counts, only Jeff Brower was also able to give information regarding different echo strengths and durations (in ten-minute intervals). Although this made such findings much less-assured, it was interesting that his results showed a noticeably increased number of stronger/longer-duration echoes consistently between $\sim 19^h40^m$ to 20^h20^m UT than further from the Draconid maximum that day, which could have implied more brighter meteors/larger particles were present over the shower's best, with a skew in favour of the pre-maximum near-peak time.

5 Conclusion

It was encouraging to see the Draconid radio results seemed to confirm nicely the visual and video findings already reported, as this helps increase our confidence for events where mainly or only radio meteor data may be available for examining other unusual meteor activity. As usual, my most grateful thanks go to everyone named above for their data and correspondence from the Draconid epoch, which have helped make this report practical.

References

Maslov M. (2011). "Future Draconid outbursts (2011 - 2100)". *WGN, Journal of the IMO*, **39:3**, 64–67.

Molau S., Kac J., Berko E., Crivello S., Stomeo E., Igaz A., and Barentsen G. (2012). "Results of the IMO Video Meteor Network – October 2011". *WGN, Journal of the IMO*, **40:1**, 41–47.

Vaubaillon J., Watanabe J., Sato M., Horii S., and Koten P. (2011). "The coming 2011 Draconids meteor shower". *WGN, Journal of the IMO*, **39:3**, 59–63.

Handling Editor: Javor Kac
This paper has been typeset from a LaTeX file prepared by the author.

Meteor science

Three components of 'Taurids'

Masahiro Koseki[1]

Observations and the estimated activity profile both show the 'Taurids' are not a single entity but consist of three showers. It is necessary to study ecliptic streams such as 'Taurids' very carefully, because they are located near the ANT area, where sporadic or minor activities continue the whole year round. Nevertheless, photographic and CCD observations show a clear dip in the activity against the background and further analysis permits the discrimination of three components at the following solar longitudes and with the following radiants and geocentric velocities:

	α	δ	V_g (km/s)	Mean $\lambda_\odot$
S_E activity	36°.5	+9°.8	28.6	202°.6
S_F activity	53°.0	+13°.9	27.0	223°.4
Northern activity	55°.5	+21°.3	28.7	226°.3

Observations might suggest other weaker activities exist but they are buried in the background activity. It is said that the 'Taurid' activity interval may extend from September to December, but the observations and analysis presented here argue against a single stream and in favor of a mixture of three independent streams and sporadic activities.

Received 2012 February 3

1 Introduction

Hoffmeister (1948) introduced 'ecliptic showers' and many minor showers have been added to this category by many researchers. However, such 'ecliptic showers' are now divided into two classes: 'established showers' and the antihelion source ANT (Rendtel & Arlt, 2008, Chapter 8). Geminids, δ-Aquariids and 'Taurids' are included in the former and other 'ecliptic showers', such as Virginids, are classified as ANT.

Many cometary and asteroidal radiants concentrate in the ANT area, as we know. We can find a 'parent body' (or parent bodies) for any meteors in this area. It is very natural there are a few parent candidates for 'Taurids'. Whipple (1940) investigated photographic 'Taurid' meteors in detail, but questions remain even now.

Observers and investigators have extended the duration of 'Taurid' activity over longer and longer, with suggestions it might be connected with the September Piscids or December χ-Orionids (e.g., Stohl & Porubcan, 1990).

Koseki (1983) and Koseki et al. (2010) suggested the autumn ANT might consist of several components and 'Taurid' activity, which occurs at the time of year when ANT is most active, might be divided into two parts, though it has been thought to be continuous. It is necessary to confirm whether the dip is apparent or real. It calls, of course, for the most careful studies, because 'Taurids' locate just in the center of ANT. In this paper we study the structure of 'Taurid' activities in three independent manners:

1. We testify the dip not only by the raw number of meteors but also by the 'Taurid' proportion relative to all ANT meteors in photographic observations.
2. We get more clear results, by using other observations, i.e., CCD data, which were carried out by different techniques and in a different epoch.
3. We confirm the observations by the author's simple theoretical model of spatial structure of meteor streams. This provides independent proof for the observational results.

[1]The Nippon Meteor Society
4-3-5 Annaka, Annaka-shi, Gunma-ken, 379-0116, Japan.
Email: geh04301@nifty.ne.jp

IMO bibcode WGN-404-koseki-taurids
NASA-ADS bibcode 2012JIMO...40..129K

2 'Taurids' by photographic observations

2.1 Classification of meteors

We cannot observe meteors without errors even in the case of photographic observations and, therefore, obtained orbits should be treated with some error range. Observational errors do not always affect the calculated orbit in the same manner. When a meteor is bright, long and slow, errors in its orbit generally decrease. However, if observational stations are located unfavorably even in such favorable occasions, the result becomes worse. The direction and size of the errors in orbits differs case-by-case, even if observations were carried out by the same stations and for the same shower.

The D-criterion (Southworth & Hawkins, 1963) has been used for discrimination of meteors, but it is based on the distance separating meteors (showers) in the four dimensional space comprising Δe, Δq, ΔI and $\Delta\Pi$: differences of eccentricity, perihelion distance, and angles between orbital planes and between lines of apsides.

Observational errors cause distortion in D-criterion space and the 'distance' does not show real similarity of orbits. Koseki et al. (2010) showed the D-criterion does not work well in some cases and the strict use of it leads us to erroneous conclusions. For example, though Southworth & Hawkins (1963) proposed that

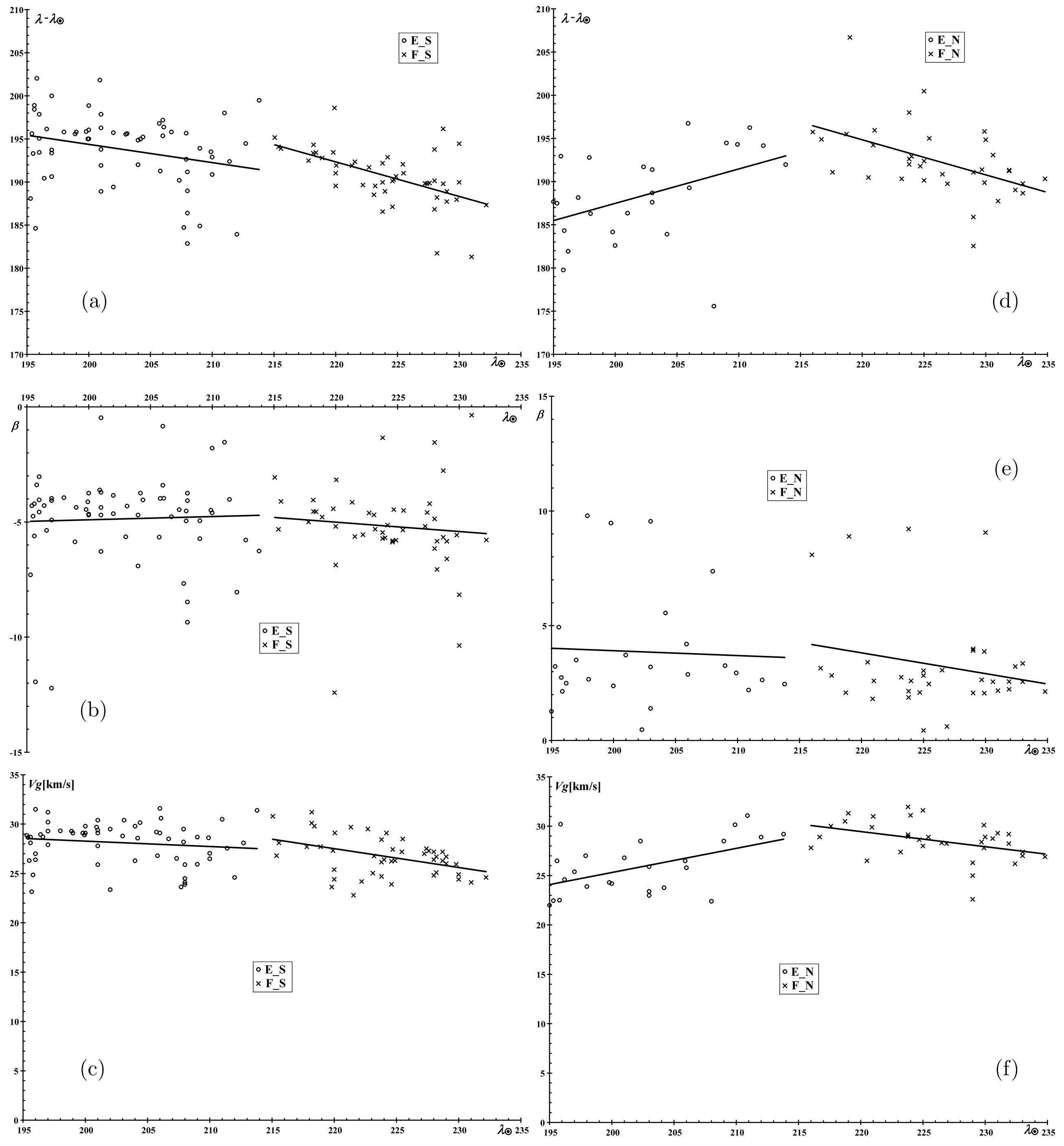

Figure 1 – Initial selection of meteors with characteristics of Taurids. Photographic meteors are selected satisfying $175 \leq \lambda - \lambda_{\odot} < 210°$, $-15 \leq \beta < +10°$, $195 \leq \lambda_{\odot} < 235°$ and $22 \leq V_g < 32$ km/s. The distributions are plotted of the ecliptic coordinates $\lambda - \lambda_{\odot}$, β and geocentric velocity with solar longitude, subdividing the data into Southern (a–c) and Northern (d–f). Separate least squares fits are shown for activity E and F, respectively below and above $\lambda_{\odot} = 215°$.

the rejection level (value of the D-criterion defining a shower) should vary inversely with the fourth root of sample size, we must not incorrectly divide a shower by reducing the discrimination level. If we use it strictly, several genuine shower members are rejected and some sporadic meteors may pollute the shower. We examine meteor shower lists later and make clear the problems caused by use of the D-criterion.

It is convenient to use observational data instead of orbital elements. We can see observational errors directly and treat them easily, whereas we cannot easily imagine a meteor position in the D-criterion's 4-dimensional space, which is distorted by observational biases.

Here we use radiant point, converted to ecliptic coordinates $(\lambda - \lambda_{\odot}, \beta)$, time of observation and geocentric velocity in order to classify meteors. These $(\lambda - \lambda_{\odot}, \beta)$ coordinates reduce the effect of radiant drift and permit us to trace a meteor shower's activity over a long enough duration.

We can refine the possible shower members by a $(\lambda_{\odot}, V_g)$ diagram (e.g., see Figure 27 of Koseki et al., 2010). Determination of velocity is the most difficult aspect of meteor observations but we can estimate the possible error range or range peculiar to a meteor shower in such diagrams. The errors in velocity may seriously distort meteor positions in D-criterion space. We therefore use $(\lambda - \lambda_\odot, \beta)$ and $(\lambda_\odot, V_g)$ diagrams for discriminating meteors.

We adopt the following area as the ANT ecliptic sources (see Koseki et al., 2010):

$$175 \le \lambda - \lambda_\odot < 210^\circ \qquad \text{and} \qquad -15 \le \beta < +10^\circ.$$

Koseki et al. (2010) suggested 'Taurids' correspond to their E and F activities (see their Figure 27). We analyze photographic data (see Table 6 of Koseki, 2009 for details of photographic data; also in Koseki, 1986) and hereafter call the activity satisfying the conditions below as activity E and F respectively:

Activity E	$195 \le \lambda_\odot < 215^\circ$	$22 \le V_g < 32$km/s
Activity F	$215 \le \lambda_\odot < 235^\circ$	$22 \le V_g < 32$km/s

We attempt to refine members of each activity by using least squares fits as shown in Figures 1(a–f). It is clear that the ecliptic coordinates $(\lambda - \lambda_\odot, \beta)$ of the radiant and geocentric velocity change with time of observations i.e., the solar longitude. We can discriminate 'Taurids' from background by differences of observed data from the least squares expressions. It seems to be proper that meteors, which satisfy the following conditions, are probable 'Taurid' candidates:

Distance of observed radiant from the least squares expressions	$\Delta r < 5^\circ$
Difference of observed velocity from the least squares expressions	$\Delta V_g < 5$ km/s

E and F activities contain Southern and Northern radiant groups. We initially divide the two groups by the sign of the radiant latitude. Figures 1(a–f) show Northern and Southern groups separately but E and F activities together. Two lines in each plot represent the least squares expressions: the left line, i.e., $\lambda_\odot < 215^\circ$ is for E activity and the right is for F activity.

2.1.1 Southern activity

Figures 1(a–c) for the Southern group suggest the two activities E and F are continuous and should be coupled as one activity. Starting from the expressions for F, which is more active than E, the possible members of Southern group are searched in all ANT meteors which are $160 \le \lambda_\odot < 270^\circ$. If a meteor is located between Northern and Southern groups, it is classified as a member of the group that is nearer, based on the distance from the estimated radiant according to the least squares expressions. We can reject sporadic meteors and add some new members. We get new expressions for refined members, but this process should be repeated till they reach convergence. Table 1 shows the results.

2.1.2 Northern activity

Figures 1(d–f) for the Northern group indicate E and F activities are two independent showers. However, starting from two separate sets of expressions, the search for possible members of each group failed. Expressions for E could not converge and showed unstable behavior if we tried to extend the expressions for E to the later period, i.e. after $215^\circ < \lambda_\odot$.

Figures 2(a) and 2(b) show the radiant distribution of E and F activity periods respectively. Northern radiants are dispersed in Figure 2(a) but have an obvious

Table 1 – The final (after the convergence process) least squares expressions and mean values for Southern activity in the period $160 \le \lambda_\odot < 270^\circ$.

n	=	123
$\lambda - \lambda_\odot$	=	$-0.2282\lambda_\odot + 241^\circ\!.2$
β	=	$-0.0296\lambda_\odot + 1^\circ\!.4$
V_g	=	$-0.1152\lambda_\odot + 52.4$
$\lambda_\odot$	=	$212^\circ\!.7$
α	=	$44^\circ\!.6$
δ	=	$11^\circ\!.1$
V_g	=	27.9 km/s
e	=	0.820
q	=	0.352 AU
i	=	$5^\circ\!.8$
ω	=	$116^\circ\!.0$
Ω	=	$32^\circ\!.7$

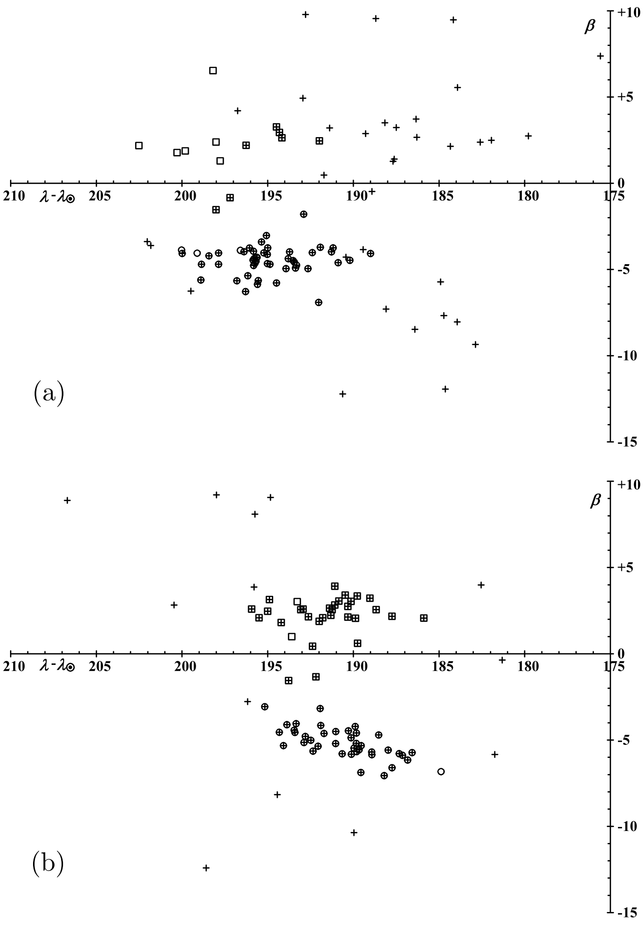

Figure 2 – The radiant distributions of (a) activity E and (b) activity F. In both figures crosses (+) represent meteors classified initially as members of activity E and F. Circles and square boxes indicate final members of respectively Southern and Northern activity after the convergence processes. Encircled or surrounded crosses are confirmed members of both activities and circles and boxes without a cross are newly added members, which have been rejected by the geocentric velocity limitation.

Table 2 – The final least squares expressions and mean values for Northern activity in the period $160 \leq \lambda_\odot < 270°$.

n	=	61
$\lambda - \lambda_\odot$	=	$-0.3093\lambda_\odot + 261.7$
β	=	$0.0049\lambda_\odot + 1.0$
V_g	=	$-0.1809\lambda_\odot + 69.6$
$\lambda_\odot$	=	226.3
α	=	55.5
δ	=	21.3
V_g	=	28.7
e	=	0.836
q	=	0.370
i	=	2.4
ω	=	292.4
Ω	=	226.3

Table 3 – The least squares expressions and mean values of Southern activities E and F.

S_E	S_F
n=47	n=40
$\lambda-\lambda_\odot$=$-0.2294\lambda_\odot + 241.3$	$\lambda-\lambda_\odot$=$-0.4069\lambda_\odot + 281.6$
β= $0.0195\lambda_\odot - 8.4$	β=$-0.0998\lambda_\odot + 17.3$
V_g=$-0.0758\lambda_\odot + 43.9$	V_g=$-0.1578\lambda_\odot + 62.2$
$\lambda_\odot$=202.6	$\lambda_\odot$=223.4
α=36.5	α=53.0
δ=9.8	δ=13.9
V_g=28.6	V_g=27.0
e=0.829	e=0.807
q=0.315	q=0.388
i=5.7	i=5.3
ω=120.7	ω=111.4
Ω=22.6	Ω=43.4

concentration in Figure 2(b). It is, therefore, proper to start from the expressions for F and to search for possible members of the entire Northern group in all ANT meteors. We can reach convergence (Table 2) through the same process as for the Southern group.

2.2 Meteor rates and three components of 'Taurids'

We count meteor rates in each 2° of solar longitude for refined 'Taurids' defined by the least squares expressions shown in Tables 1 and 2. Meteor rates in Figure 3 are the portions in percentage to all recorded meteors in the same period. The lines are smoothed by a moving average with a 10° bin; solid line is for Southern activity, dotted line is for Northern activity and dashed line is for the total. It is clear the Southern activity has two peaks, despite the initial least squares fits for the two activity periods E and F (Figures 1(a–c)) appearing similar. Northern activity, on the other hand, has one peak, even though Figures 1(d–f) suggested the possibility of two showers. The 'Taurids' therefore consist of three components – two Southern and one Northern. We will confirm this by other observations (i.e., by CCD) and by consideration of the encounter condition in subsequent sections.

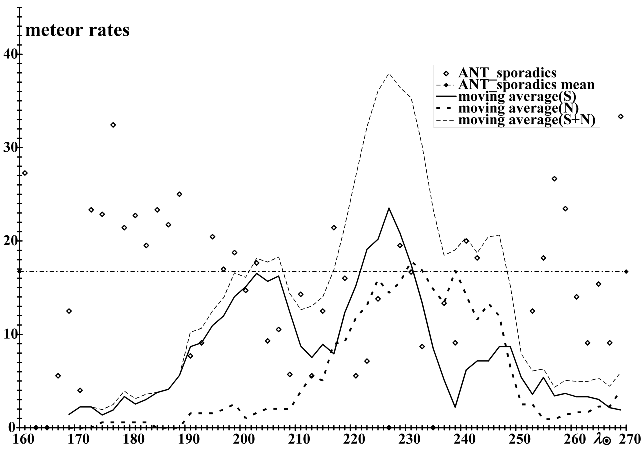

Figure 3 – The observed proportion of 'Taurids' (Southern, Northern and combined), and of ANT sporadics, to all recorded photographic meteors. We can divide all the recorded meteors into four groups, Northern activity, Southern activity, remaining ANT meteors (= ANT sporadics), and others.

There might be one more Taurid component active after $\lambda_\odot > 240°$ but it is below sporadic rates shown in Figure 3 as rhombi. Searches for smaller meteor activities than the main three in the ANT area should be carried out very carefully. The only certain result is that the 'Taurids' have the three components corresponding to the one Northern and two Southern activity peaks shown clearly in Figure 3.

2.3 Two Southern activities

We noticed E and F activities in 'Taurids' period and confirmed that Southern activity consists of two, abbreviated hereafter S_E and S_F. It is necessary to start again from Figure 1(a–f) and to reach convergence. Applying the line in Figure 1(a–c) to meteors in the period of $195 \leq \lambda_\odot < 215°$ and the line in Figure 1(d–f) to those of $215 \leq \lambda_\odot < 230°$ (we need to apply these processes for both Northern and Southern activities together, because the discrimination between Northern and Southern affects the final results), we can again discriminate stream members from sporadics based on the difference from estimated radiant point and velocity. We reach the result shown in Table 3 through the similar convergence process described above.

The radiants of these two activities are very close at the solar longitude $\lambda_\odot$=215° where they overlap (Figure 1(a–c) and see Appendix). Visual observers can record only the dip in the activities and cannot discriminate them by radiant points. Even if we have orbital data, we could not discriminate between both components and from the sporadic background also. Table 3 gives the converged results based on the activity dip only, i.e., divided by $\lambda_\odot$=215°. However, CCD observations and consideration of the encounter condition support this separation.

3 'Taurids' by CCD observations

Applying photographic convergence values (Tables 1 and 2), meteor rates counted in SonotaCo data (SonotaCo, 2010) for Southern and Northern activities are plotted

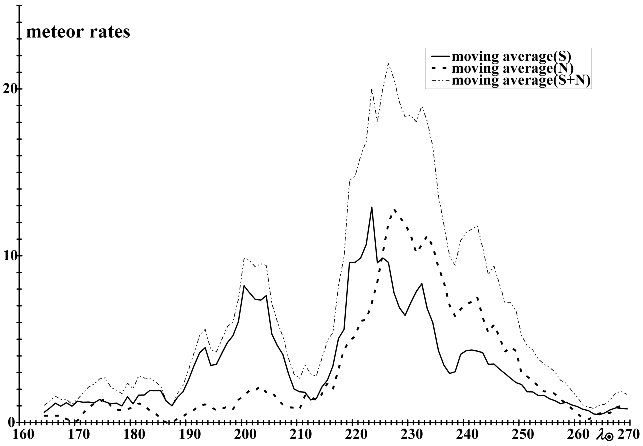

Figure 4 – The observed proportion of 'Taurids' to all meteors as recorded by CCD.

in Figure 4. It is clear that there exist three components of 'Taurids', that is, two Southern and one Northern activity. Another activity $\lambda_\odot > 240°$ is suggested again, but it is very difficult to confirm a certain shower in ANT area even though the amount of CCD data is much larger than photographic. Very careful investigation is necessary to distinguish this new candidate shower from sporadics, S_F and Northern components. It remains as a puzzle for future work.

4 Estimation of meteor activity profile based on simple meteor stream model

It is sufficiently reliable to assume these two hypotheses (Koseki, 1975, 2012):

1. The axis of a meteoroid orbit remains the same as the parent body (or the center of the stream).
2. The apsides of the meteoroid orbit, or the semi-major axis, is kept at the same size.

We may then estimate each of the three components of 'Taurid' activity by using mean orbital data shown in Tables 2 and 3. We need to standardize estimations of the three components in order to compare the observed (proportion) rates of 'Taurids'. Judging from Figures 3 and 4, the activity level of the Northern component is roughly equal to S_F but S_E is less than they are. It might be appropriate to assume that the peak estimated rates are 8, 8 and 5, respectively for Northern component, S_F and S_E. It is also necessary to normalize the observed rates of photographic and CCD in order to compare them with the estimations. The 'Taurids' proportion of photographic is higher than of CCD, about twice (Figures 3 and 4). It is proper to normalize the peak rates (of the three model components combined) to observed rates around $\lambda_\odot \sim 224°$ and to examine whether the model fits the observations at other values of $\lambda_\odot$.

Figure 5 shows the result. Fine solid lines represent the model estimates for each component: crosses, asterisks and triangles show Northern component, S_F and S_E respectively. The thick line with small circles is the total estimated rates of all three components. The solid line without marks is photographic rates and the dotted line is CCD rates, which are normalized to the peak of total estimated rates: both lines are shown by a smoothed line, using a moving average of 10° and 5° in $\lambda_\odot$ respectively.

The total rates estimated from the model represent the observed changes of activities very well for both photographic and CCD. Observed rates obtained by both methods deviate from the estimated rate after $\lambda_\odot > 238°$ and suggest again another activity more positively.

5 Discussion

5.1 Sporadic background and 'Taurids'

Sporadic meteor activity is conspicuous everywhere in ANT area. We must evaluate the influence of sporadic meteors on our three components of 'Taurids'. Figure 3 shows the meteor rates of the remaining ANT meteors after omitting members of our three components. Rhombi in Figure 3 give the proportion of such 'ANT sporadic' meteors and the horizontal line shows their mean. The proportion of sporadic meteors seems to decrease during the period of 'Taurids'.

Even refined 'Taurid' members are contaminated by sporadic meteors, because sporadics are distributed in the center of 'Taurids'. It is natural there is some uncertainty of the data listed in Tables 1–3. We cannot discriminate between 'Taurid' and sporadic meteors individually and must treat the data statistically. Activity profiles give us another view on the contrast of 'Taurids' with the sporadic background.

There are three recognizable peaks in Figure 3 above the background meteors and they are verified in Figure 4. If we considered the decrease of the sporadic portion during 'Taurids', the activities of each of our three components might not reach the sporadic level. The total activity of the three (moving average (S+N) in Figure 3) exceeds the background activity and we can recognize only the total 'Taurids' by visual observations.

It is very difficult to classify ANT meteors into exact categories, even if their paths were plotted. Ordinary visual observers can count the total number of

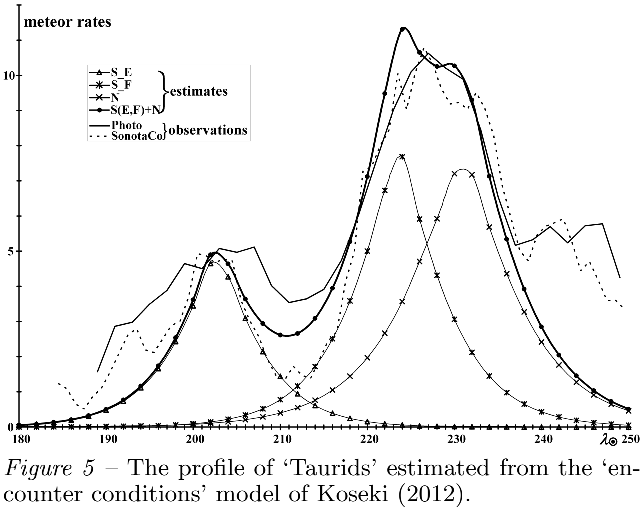

Figure 5 – The profile of 'Taurids' estimated from the 'encounter conditions' model of Koseki (2012).

Table 4 – 'Taurids' and related activities in photographic data detected by cluster analysis (Koseki, 1983). The second line of each entry shows the derivative with respect to the solar longitude of observations $\lambda_\odot$.

No.	α	δ	$\lambda - \lambda_\odot$	β	V_g	e	q	i	ω	Ω	n
1	34.2	+8.9	196.5	−4.4	28.9	0.835	0.290	6.0	124.2	18.4	48
	0.72	0.26	−0.24	0.01	−0.01	0.0002	0.0031	−0.05	−0.50		
2	54.0	+13.9	189.9	−5.3	26.3	0.797	0.406	5.4	109.5	45.1	49
	0.62	0.09	−0.39	−0.05	−0.17	−0.0021	0.0070	−0.03	−0.86		
3	56.6	+21.9	191.5	+2.1	28.7	0.845	0.356	2.5	293.6	227.7	36
	0.73	0.13	−0.32	−0.02	−0.18	−0.0024	0.0060	−0.06	−0.71		
4	32.7	+10.8	191.6	−2.2	25.7	0.779	0.387	2.4	113.5	22.6	15
	0.78	0.07	−0.26	−0.19	0.06	0.0022	0.0027	0.20	−0.55		
5	20.1	+3.2	194.1	−4.9	27.2	0.809	0.341	5.7	118.9	5.7	13
	0.57	0.30	−0.37	0.07	0.14	0.0046	0.0030	−0.09	−0.74		

'Taurids' only and they regard 'Taurids' as continuing over a month. The visual profile of 'Taurids' gives the total 'Taurids' including contamination from the sporadic background. If we intend to decrease the interference, we need to plot meteor paths. In the cases of photographic and CCD observations, we can distinguish three components and their activity profiles separately. Radar observations can offer a much larger amount of data than photographic and CCD, but their results are problematic. We examine how different observational methods affect our view of meteor showers in the next section.

5.2 Observational methods and 'Taurids'

It is necessary to note that the results we have found here do not concern radar data but photographic and CCD observations. Different results have been obtained by different methods. At first, we review the author's previous research on photographic data by using the centroid method of cluster analysis (Koseki, 1983). Summary results are given in Table 4 and it is evident that three components of 'Taurids' are clearly found by optical observations. Nos. 1–3 of Table 4 coincide with S_E, S_F and Northern components of this study. It was suggested also:

1. No. 1 of Table 4 seems to be independent and to have no related Northern branch. It has been said any ecliptic shower consists of two, that is, Northern and Southern branches. It is not so: there might be many independent showers.

2. The Taurids and related activities do not seem to come from only one common parent body, such as 2P/Encke.

It is uncertain whether No. 4 of Table 4 is a subcenter of No. 1 or a chance association. There are many smaller activities detected by Koseki (1983) in addition to No. 5, which might correspond to 'Piscids', and very careful studies are necessary to confirm their reliability.

The author made another study by using cluster analysis among published lists of radar and of photographic showers, in total 1894, and he discovered 223 clusters in total (Koseki, 1981). Five clusters, i.e., five meteor streams, might be related to 'Taurids'. [This survey and the above-mentioned cluster analysis (Koseki, 1983) are summarized in an English paper (Koseki, 1986). The 223 clusters are divided into 255 showers, because twin showers are included in the 223, and published in WGN (Table 5 of Koseki, 2009).] The results are shown in Table 5 which consists mainly of radar observations except for two optical (photographic) observations, i.e., L1-31 and L1-61. We can therefore obtain a radar view of 'Taurids' through Table 5.

Of the clusters in Table 5, No. 12 is more active as the daytime shower (ζ-Perseids) than the night-time Piscids-Arietids. The latter is near our S_E component. No. 19 and No. 27 both have daytime β-Taurids but the name of β-Taurids has been used in confusion because of its weaker activity than of ζ-Perseids. No. 20 and No. 27 both include Northern and Southern 'branches' of 'Taurids', because the classification becomes more difficult in the fainter meteor range. No. 20 is a mixture of S_F and Northern components. It is suggested that No. 27 is a combination of S_E and S_F. No. 48 might be a candidate for the later activity $\lambda_\odot > 240°$.

It is clear apparent similarity of orbits does not always lead us to the right conclusions. The cluster analysis using the D-criterion combines radar daytime streams with optical ones mechanically without consideration of the differences of meteoroids and of errors. How to classify meteors is crucial for studying meteor stream structure, but the operations are often carried out mechanically even in the original investigations. Figure 6 shows the perihelion distributions of our three components with the five related 'Taurid' groups. We see the confusion of classification clearly in the perihelion distributions. These five groups are made up only by the similarity of orbits and a group does not necessarily have a common origin. Therefore, Koseki (2009) described the list of the groups as the 'reference list' of meteor streams.

The different characteristics highlighted by different observational techniques, i.e., brightness of meteors, are stressed by Koseki (2009) and Koseki et al. (2010). It is very natural that there might be another view from a different brightness range and from a different epoch of observations. The level of a meteor shower relative to all meteors differs depending on brightness. It is well known that the relative level of a meteor shower reduces in fainter ranges in many cases. We know activity levels of meteor showers change from year to year and some

Table 5 – Clusters/streams related to 'Taurids' identified primarily in radar data. The Table shows:
The original numbers of Koseki (1981): Nos. 12, 19, 20, 27 and 48.
The numbers in WGN (Koseki, 2009, Table 5) are listed in parentheses: such as 66, 165. All five candidates are twin showers and they are given two numbers in WGN, one daytime and the other night-time. We can identify each twin by the ecliptic coordinates: daytime showers are near the helion source ($\lambda - \lambda_\odot \sim 360°$) and night-time showers near ANT.
Mean elements of the group.
Following lines show individual observations, in which abbreviations (Ref.-No.) used here are the same as in WGN (Koseki, 2009, Table 5). Note that shower names in remarks are given by the original authors.

No. 12 (66, 165)		$e = 0.790$		$q = 0.355$		$i = 2.9$		$\omega = 80.0$		$\Omega = 54.2$	
Ref.-No.	α	δ	$\lambda - \lambda_\odot$	β	V_g	e	q	i	ω	Ω	Remarks
K1-40	41.0	23.0	351.6	6.8	27.0	0.770	0.440	6.0	74.0	54.0	
K1-42	52.0	23.0	344.4	4.0	30.0	0.800	0.310	6.0	57.0	71.0	ζ-Perseids
LE-191	47.2	14.9	350.7	−2.6	29.3	0.820	0.400	2.9	250.1	238.2	
LE-244	61.0	21.5	345.6	0.7	23.5	0.780	0.340	0.7	59.2	77.6	ζ-Perseids
LE-245	62.8	26.0	346.5	4.8	24.8	0.690	0.410	4.3	61.5	79.2	
S2-38	60.2	24.8	345.5	4.1	28.6	0.834	0.319	5.3	59.2	77.6	ζ-Perseids
S3-74	63.3	27.1	345.5	5.8	25.1	0.755	0.365	6.5	60.5	80.8	ζ-Perseids
NI-610502	46.5	19.1	347.3	1.6	24.4	0.750	0.390	2.9	64.8	62.1	
NI-610603	64.2	25.4	343.0	4.0	28.4	0.820	0.300	5.7	55.4	83.8	ζ-Perseids
K1-149	27.0	9.0	193.3	−2.0	31.0	0.840	0.330	2.2	118.0	15.0	Taurids(S)
S2-58	23.9	8.8	197.6	−1.1	29.2	0.841	0.273	1.4	126.9	7.8	Arietids(S)
S3-232	32.3	10.2	195.8	−2.7	25.6	0.768	0.333	2.9	122.5	17.8	Arietids(S)
L1-31	26.0	14.0	190.1	3.0	29.0	0.797	0.399	3.4	290.8	199.1	Piscids
No. 19 (73, 170)		$e = 0.830$		$q = 0.357$		$i = 7.8$		$\omega = 261.0$		$\Omega = 240.0$	
Ref.-No.	α	δ	$\lambda - \lambda_\odot$	β	V_g	e	q	i	ω	Ω	Remarks
K1-80	64.0	15.0	346.8	−6.2	31.0	0.850	0.340	7.0	243.0	258.0	β-Taurids
LE-247	64.4	11.5	347.6	−9.7	29.3	0.800	0.370	11.0	244.9	257.0	β-Taurids
K1-179	33.0	18.0	191.9	4.4	30.0	0.840	0.360	5.5	295.0	205.0	Taurids(N)
No. 20 (77, 194)		$e = 0.775$		$q = 0.493$		$i = 0.5$		$\omega = 92.6$		$\Omega = 67.8$	
Ref.-No.	α	δ	$\lambda - \lambda_\odot$	β	V_g	e	q	i	ω	Ω	Remarks
K1-77	73.0	19.0	357.9	−3.5	24.0	0.710	0.560	2.0	265.0	256.0	
LE-250	70.8	28.8	355.3	6.5	25.2	0.730	0.510	5.3	80.0	77.8	
LE-252	76.1	16.9	357.7	−5.9	25.9	0.770	0.540	4.8	264.9	258.9	
NI-610605	75.5	20.3	352.2	−2.5	25.5	0.790	0.460	3.7	255.1	264.2	
LE-568	60.2	22.4	188.6	1.7	30.3	0.850	0.400	1.8	287.0	234.0	Taurids(N)
LE-642	64.9	14.7	184.4	−6.6	26.9	0.790	0.500	5.7	97.3	61.2	Taurids(S)
LE-643	65.4	24.9	186.6	3.3	27.8	0.800	0.460	3.1	282.2	241.2	Taurids(N)
LE-704	74.4	17.8	176.5	−4.8	24.7	0.780	0.610	3.4	81.8	78.6	
S1-2	59.7	19.2	191.8	−1.3	25.5	0.770	0.385	1.4	114.1	49.7	Taurids
NI-611101	59.0	16.6	184.3	−3.7	23.8	0.760	0.500	4.2	99.0	56.1	Taurids(S)
No. 27 (85, 179)		$e = 0.823$		$q = 0.333$		$i = 1.3$		$\omega = 100.2$		$\Omega = 50.7$	
Ref.-No.	α	δ	$\lambda - \lambda_\odot$	β	V_g	e	q	i	ω	Ω	Remarks
LE-249	68.3	23.4	352.3	1.4	28.6	0.810	0.430	1.4	73.2	77.9	
S2-43	79.4	21.2	345.6	−1.9	28.2	0.825	0.325	2.2	239.2	274.5	β-Taurids
S3-102	83.9	23.6	342.4	0.3	29.0	0.834	0.274	0.3	52.3	102.0	β-Taurids
K1-160	40.0	15.0	200.3	−0.6	33.0	0.860	0.240	1.2	131.0	22.0	Taurids(S)
LE-520	41.0	11.4	191.9	−4.3	29.7	0.820	0.360	4.9	114.1	30.2	Taurids(S)
LE-521	42.3	18.4	195.0	2.0	31.8	0.850	0.300	2.8	301.2	210.4	Taurids(N)
S3-250	46.3	17.4	191.6	0.0	24.6	0.750	0.398	0.0	293.6	217.2	Taurids
L1-61	40.0	13.0	193.0	−2.5	31.0	0.828	0.330	3.3	118.8	28.7	Taurids
NI-611001	44.8	12.4	193.0	−4.4	28.8	0.830	0.340	5.9	118.3	33.0	Arietids(S)
No. 48 (52, 193)		$e = 0.737$		$q = 0.583$		$i = 1.4$		$\omega = 88.0$		$\Omega = 57.7$	
Ref.-No.	α	δ	$\lambda - \lambda_\odot$	β	V_g	e	q	i	ω	Ω	Remarks
LE-192	51.6	23.5	356.3	4.6	25.2	0.740	0.520	3.8	82.1	58.8	
LE-193	59.1	17.8	2.2	−2.6	24.6	0.770	0.600	1.8	273.3	238.5	
S3-59	43.6	20.9	359.9	4.1	20.6	0.708	0.592	2.8	90.0	47.4	ε-Arietids
NI-610505	58.8	23.7	359.3	3.3	21.0	0.710	0.600	2.7	89.5	62.3	
LE-567	52.0	20.8	180.8	1.9	23.2	0.690	0.580	1.4	270.9	234.0	
LE-639	57.5	21.0	178.1	0.9	24.2	0.750	0.600	0.7	265.1	241.8	
LE-641	58.4	14.3	178.2	−5.8	25.2	0.790	0.590	4.2	85.1	61.1	

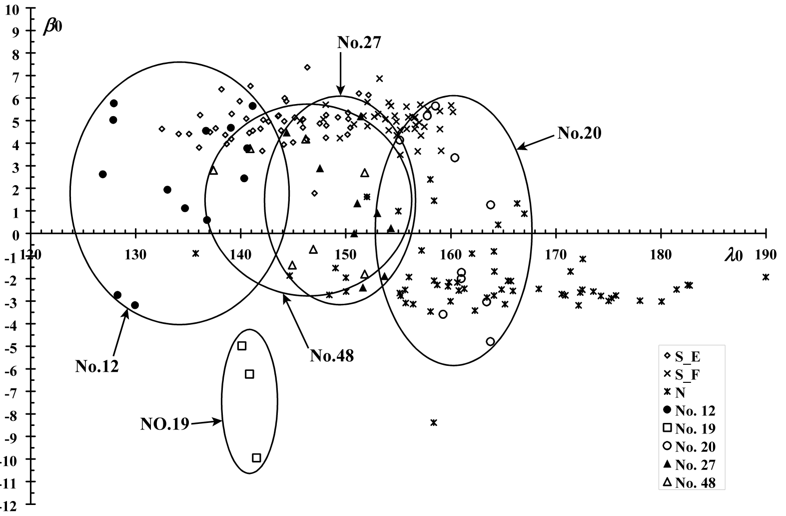

Figure 6 – Perihelion distribution, in ecliptic coordinates, of five related 'Taurid' groups (Table 5), and of Northern, S_E and S_F 'Taurid' components found in the present work. For the five groups, each observation (i.e., originally observed showers) is plotted, and for the three components, all photographic data are given.

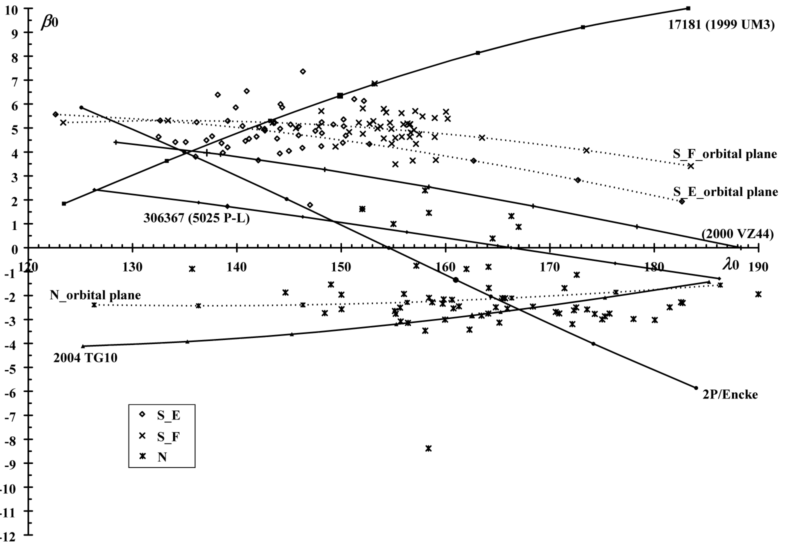

Figure 7 – Perihelion distribution of the three components of 'Taurids' and parent body candidates.

showers might be observable only periodically or on occasions.

Photographs and CCDs record bright meteors, which can be seen by the naked eye, and three components of 'Taurids' could be caught by careful visual observers plotting meteor paths on charts. Radar results could not be observable by eye and optical observations could not always be confirmed by radar.

5.3 Parent bodies and 'Taurids'

We used the simple model, which is based on the hypothesis that the line of apsides of the stream is approximately preserved over long intervals, and determined the classification by means of observed data, in other words, radiants and geocentric velocity. We did not use the similarity of orbits, i.e., D-criterion, which includes the deviation from the mean apsides in calculations, in order to discriminate meteors. The distribution of the perihelia of every meteor belonging to each of the three components could test our model and give suggestions as to their origin.

Figure 7 shows the unique structure of 'Taurids'. Koseki et al. (2010) pointed out interesting features of 'Taurids' perihelia:

1. The perihelion distribution is elongated along the ecliptic plane, suggesting Taurids' orbital plane rotates about the ecliptic axis, not 2P/Encke's.
2. The perihelion of 'Northern branch' at the maximum almost coincides with 2P/Encke's.
3. The perihelion of 'Southern branch' at the maximum recedes gradually from 2P/Encke's.

This appearance looks curious, if we regarded 'Taurids' as a single stream or originating from the same celestial body. If 'Taurids' are not one but consist of three independent showers, that distribution is very natural:

1′. If we would accept Southern activities are not the descendant of 2P/Encke, their perihelia are independent from the comet's.

2′. The perihelia of Northern meteors are distributed around that of 2P/Encke and along its orbital plane, though it is necessary to note that Northern activity could not be clearly limited in terms of $\lambda_\odot$ and might be polluted by sporadic meteors especially towards both ends. The perihelia of some meteors discriminated as 'Northern' activity distribute above the ecliptic plane, i.e., $\beta > 0$ and, therefore, their radiants locate under the ecliptic.

3′. The perihelion does not recede but perihelia of two independent Southern showers are situated 10° apart. Though two concentrations of the perihelia are not so clear, we can recognize two activities by meteor rates.

Koseki et al. (2010) suggested the perihelia of shower meteors locate along the orbital plane of its parent body. They gave figures for Leonids, Perseids and the twin pair Orionids and η-Aquariids. Their Leonid and Perseid figures represent clearly the perihelia distributions along the plane, though the twin shows a somewhat different appearance because of observational errors. Some candidates of 'Taurids' parent bodies (Rendtel & Arlt, 2008) are shown in Figure 7 with their orbital planes. It seems that perihelia of 'Taurid' meteors are distributed along their own average orbital plane (dotted lines). The perihelia of Northern activity meteors seem to be on the orbital plane of 2P/Encke, as mentioned above. Only 2004 TG_{10} has a plausible orbital plane for the parent body of Northern activity. We see no good candidate for both S_E and S_F activities now, but there might be many unknown near Earth objects. It is not necessary to regard 2P/Encke as the only candidate of 'Taurids', because the rotation of the ascending node caused by Jupiter's perturbation requires several thousand years to produce Northern and Southern branches. There might be many other hypotheses.

5.4 Estimated profile and 'Taurids'

Koseki (2011, 2012) published similar studies concerning meteor activity profiles based on the simple model of a meteor stream and showed the estimated profile can proffer another clue for studying meteor activity against the background. This estimation does not need a heap of orbital data nor a sophisticated technique to calculate orbital evolution. Only mean orbital elements and an observed profile of a meteor shower make it possible to testify whether and when a meteor shower is active. 'Taurids' are an excellent case for showing the usefulness of estimation by the simple model.

Figure 5 clearly shows that the simple model works well even for ecliptic streams such as 'Taurids' and that 'Taurids' is not one but consists of three showers. The total of the model estimated rates expresses the features of observed meteor rates down to every detail:

1. The hollow around $\lambda_\odot \sim 212°$ is explained by the gap between the activity S_E and S_F.
2. Activities of two components represent the maximum of 'Taurids' around $\lambda_\odot \sim 226°$ that coincides with the well known date for Taurids.
3. The Northern component is active later and longer than the Southern one, and extends the total 'Taurids' activity.

Though we have not selected member meteors of the three components from the simple model, the variations of meteor rates selected independently by the least squares method agree well with the model estimation. The simple model strengthens our argument for three showers of 'Taurids'.

6 Conclusions

1. The concept of 'Taurids' should be refined. Three independent meteor activities are confirmed even though sporadic meteors are abundant.
2. The simple model of a meteor shower is very useful to understand meteor activity variations. Meteor activity does not continue over a month even for ecliptic showers.
3. Optical observations (visual, photographic, CCD) can detect 'Taurids' but the presence of meteor activity differs between observational methods.

References

Hoffmeister C. (1948). *Meteorströme*. Johann Ambrosius Barth Verlag, Leipzig.

Koseki M. (1975). "A simple model of a meteor stream structure". *16th Japanese Meteor Conference*. (In Japanese).

Koseki M. (1981). "Cluster analysis on 1894 meteor showers". *22nd Japanese Meteor Conference*. (In Japanese).

Koseki M. (1983). "Photographic Taurids". *24th Japanese Meteor Conference*. (In Japanese).

Koseki M. (1986). "Analysis of meteor data on a microcomputer system". *J. Brit. Astron. Assoc.*, **96**, 232–240.

Koseki M. (2009). "Meteor shower records: A reference table of observations from previous centuries". *WGN, Journal of the IMO*, **37:5**, 139–160.

Koseki M. (2011). "Coma Berenicids and related activities". *WGN, Journal of the IMO*, **39:6**, 159–166.

Koseki M. (2012). "Encounter conditions of meteor streams and their activity profiles—a simple model of spatial structure of meteor streams". *WGN, Journal of the IMO*. In press.

Koseki M., Ueda M., and Shigeno Y. (2010). "What is the difference between image intensifier and CCD meteors? III. How do meteor showers look like by image intensifiers and by CCD?". *WGN, Journal of the IMO*, **38:5**, 145–160.

Rendtel J. and Arlt R., editors (2008). *Handbook for Meteor Observers*. IMO, Potsdam.

Table 6 – Radiant drifts of Northern component and Southern activity.

Northern activity																							
$\lambda_\odot$	160	165	170	175	180	185	190	195	200	205	210	215	220	225	230	235	240	245	250	255	260	265	270
α	10.5	13.7	16.9	20.2	23.4	26.7	30.0	33.4	36.8	40.2	43.6	47.1	50.7	54.3	57.9	61.6	65.2	69.0	72.7	76.5	80.3	84.1	87.9
δ	6.4	7.8	9.1	10.5	11.8	13.0	14.3	15.4	16.6	17.7	18.7	19.7	20.7	21.5	22.3	23.0	23.7	24.2	24.7	25.1	25.4	25.6	25.7

Southern activity																							
$\lambda_\odot$	160	165	170	175	180	185	190	195	200	205	210	215	220	225	230	235	240	245	250	255	260	265	270
α	5.7	9.3	12.9	16.5	20.1	23.8	27.4	31.1	34.8	38.6	42.4	46.2	50.0	53.9	57.8	61.7	65.6	69.6	73.6	77.6	81.6	85.6	89.6
δ	−1.2	0.2	1.6	2.9	4.2	5.5	6.8	8.0	9.1	10.2	11.2	12.2	13.1	13.9	14.6	15.2	15.7	16.2	16.5	16.8	16.9	16.9	16.8

SonotaCo (2010). "SonotaCo Network simultaneously observed meteor data sets". `http://sonotaco.jp/doc/SNM/` .

Southworth R. B. and Hawkins G. S. (1963). "Statistics of meteor streams". *Smithson. Contrib. Astrophys.*, **7**, 261–285.

Stohl J. and Porubcan V. (1990). "Structure of the Taurid meteor complex". In Lagerkvist C.-I., Rickman H., Lindblad B. A., and Lindgren M., editors, *Asteroids, Comets, Meteors III*, pages 571–574. Uppsala Universitet.

Whipple F. L. (1940). "Photographic meteor studies. III. The Taurid shower". *Proc. Amer. Phil. Soc.*, **83**, 711–745.

Table 7 – Radiant drifts of two Southern components.

S_E component										
$\lambda_\odot$	185	190	195	200	205	210	215	220	225	230
α	23.9	27.4	31.0	34.6	38.3	42.0	45.7	49.5	53.3	57.2
δ	4.8	6.3	7.7	9.1	10.4	11.7	12.9	14.0	15.1	16.0

S_F component									
$\lambda_\odot$	205	210	215	220	225	230	235	240	245
α	41.7	44.8	47.8	50.9	54.0	57.1	60.1	63.2	66.3
δ	12.7	13.1	13.4	13.7	14.0	14.2	14.3	14.3	14.4

Table 8 – The least squares expressions and mean values of Southern and Northern activities by CCD observations.

Southern activity	Northern activity
n=1119	n=1040
$\lambda-\lambda_\odot=-0.2083\lambda_\odot+237.6$	$\lambda-\lambda_\odot=-0.1853\lambda_\odot+233.9$
$\beta=-0.0239\lambda_\odot+0.3$	$\beta=-0.0085\lambda_\odot+4.5$
$V_g=-0.0953\lambda_\odot+48.1$	$V_g=-0.1098\lambda_\odot+52.7$
$\lambda_\odot$=221.5	$\lambda_\odot$=230.4
α=52.2	α=59.3
δ=13.0	δ=22.2
V_g=27.0	V_g=27.4
e=0.804	e=0.815
q=0.378	q=0.375
i=5.5	i=2.9
ω=113.0	ω=292.7
Ω=41.5	Ω=230.4

Appendix: Radiant drift of three 'Taurid' meteor activities

We can calculate radiant drifts using Tables 1–3. Table 6 shows calculated radiant drifts for Northern and Southern activities based on Tables 1 and 2, though the activity profile reveals they are a conglomerate of three. Radiant drifts in Table 6 coincide well with observations around the maximum. We may see meteors radiating from the indicated area but a noticeable fraction, especially away from the maximum, may be sporadic.

We cannot exclude contaminations from sporadic meteors and their proportion increases away from the maximum. We note that they show the false radiant of so-called 'Taurids', which is a conglomerate of sporadic and minor shower meteors, apart from the maximum.

We find two Southern components, though we could not divide them by radiant distribution. If we divided them based on time intervals, we can get radiant drifts for S_E and S_F components individually from Table 3. Table 7 shows the estimated radiant drifts extended over the searched intervals for comparison and it is clear that radiants of two activities in $205 \le \lambda_\odot < 230°$ could not be separated visually. We do not intend to give exact radiant positions, because the converged expressions are not obtained so accurately owing to the influence of sporadic contaminations. We note that two showers seem to be one in radiant position but in fact they are independent showers.

We can get similar drifts from the least squares expressions of CCD observations by repeating similar processes as in the case of photographic data in order to get convergence. Table 8 shows the results and it may be thought that there are rather large differences between photographic and CCD. If we apply the converged expressions to restricted intervals near the maximum, both photographic and CCD results coincide very well for Northern and Southern activities.

The difference in radiant position between photographic and CCD becomes larger away from the maximum. The converged data are calculated for meteor activities of ANT area in the period $160 \le \lambda_\odot < 270°$, though our three components of 'Taurids' are active for no more than a month. The difference between photographic and CCD shows the dispersed 'Taurids' activity, that is, ANT background activity and not an independent shower.

We could not calculate the least squares expressions for S_E and S_F components individually, because there are gaps in CCD observations though they have a much larger amount of data overall than photographic.

Handling Editor: David Asher

Preliminary results

Results of the IMO Video Meteor Network — April 2012

Sirko Molau[1], *Javor Kac*[2], *Erno Berko*[3], *Stefano Crivello*[4], *Enrico Stomeo*[5], *Antal Igaz*[6] *and Geert Barentsen*[7]

The 2012 April report for the IMO Video Meteor Network is presented. More than 12 000 meteors were recorded by 64 cameras in over 5 200 hours of effective observing time. The Lyrids peaked on April 21 at 02^h UT based on Network data. The ν-Cygnids were confirmed and the shower parameters improved. The δ-Aquilids and σ-Leonids were clearly detected, however their radiant positions differ somewhat from those in the MDC list. The Southern May Ophiuchids can be traced from April 15 to June 6. The activity drift could be split into two segments, possibly hinting on two separate showers. The April χ-Librids were also detected, essentially confirming shower parameters from the MDC list.

Received 2012 June 13

1 Introduction

April 2012 was the first month since January 2010 where we recorded fewer meteors than in the same month of the preceding year. This happened because April 2011 had presented almost perfect weather conditions to the observers, whereas this April was mediocre at best. Hence, only 17 of the 64 active cameras managed to observe in twenty or more nights. On the other hand, the weather was quite fair, as there was hardly any camera with less than ten observing nights. So this time no observer was given an advantage or disadvantage. Overall we collected about 5 200 hours of effective observing time in those thirty April nights, and recorded 12 200 meteors (Table 7 and Figure 1).

Two new camera systems were installed in Germany in April. At the balcony of his house south of Berlin, Rainer Arlt started to operate Ludwig1, and used Sony camera equipped with an 8 mm $f/0.8$ Computar lens. One day the camera will probably be replaced by a more powerful system. Also the field of view still has to be synchronized such that Ludwig1 operates together with Remo1 in Ketzür and Armefa in Berlin-Treptow in a multi-station mode.

Jörg Strunk upgraded his old Mincam4 camera, which was only used to determine the appearance times of fireballs to date. He replaced the fisheye lens by a 2.6 mm $f/1.0$ Computar lens. Now the accuracy and limiting magnitude is just sufficient for the IMO camera network.

[1]Abenstalstr. 13b, 84072 Seysdorf, Germany. Email: sirko@molau.de
[2]Na Ajdov hrib 24, 2310 Slovenska Bistrica, Slovenia. Email: javor.kac@orion-drustvo.si
[3]Bercsenyi ut 3, 3188 Ludanyhalaszi, Hungary. Email: berko@is.hu
[4]Via Bobbio 9a/18, 16137 Genova, Italy. Email: stefano.crivello@libero.it
[5]via Umbria 21/d, 30037 Scorze (VE), Italy. Email: stom@iol.it
[6]Húr u. 9/D, H-1223 Budapest, Hungary. Email: antaligaz@yahoo.com
[7]University of Hertfordshire, Hatfield AL10 9AB, United Kingdom. Email: geert@barentsen.be

IMO bibcode WGN-404-molau-vidapr
NASA-ADS bibcode 2012JIMO...40..139M

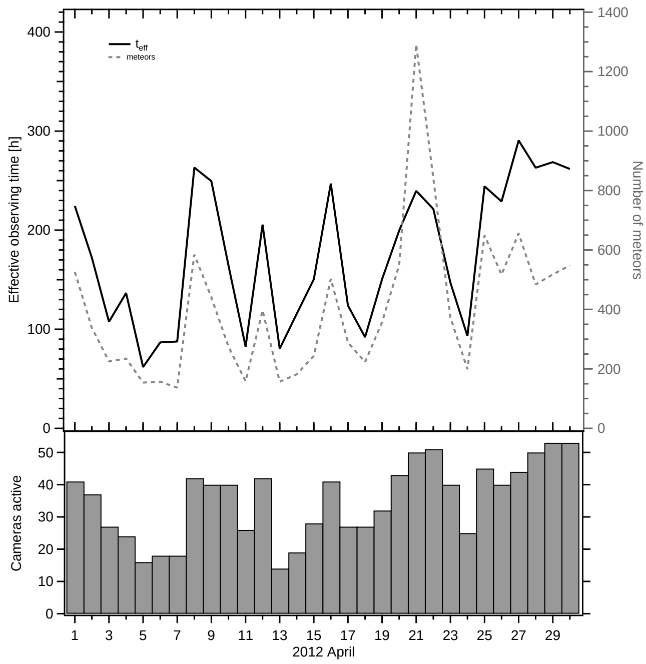

Figure 1 – Monthly summary for the effective observing time (solid black line), number of meteors (dashed gray line) and number of cameras active (bars) in 2012 April.

2 Lyrids

The most important meteor shower of April are the Lyrids. Their maximum was predicted for the morning hours of April 22 and matched perfectly to the new Moon – ideal observing conditions if also the weather would be cooperative. Overall there were not many places with clear skies all night long, but April 21/22 was at least one of the more successful nights with fifty active cameras. Figure 2 shows the most interesting part of the activity profile between April 20 and 24, based on 1 600 Lyrids. The activity rose in the European evening hours of April 21 and reached at the next morning at 02^h UT a peak with about 5 meteoroids per 1 000 km^2 per hour (equivalent to a ZHR of 20). Thereafter the activity seemed to decline again, but that cannot be stated with full certainty, as there is a larger gap after the European night time hours.

Visual observers could fill in this gap much better.

Table 1 – Parameters of the Lyrids from the MDC Working List and the IMO Network analysis in 2012.

Source	Solar Longitude		Right Ascension		Declination		V_∞	
	Mean [°]	Interval [°]	Mean [°]	Drift [°]	Mean [°]	Drift [°]	Mean [km/s]	Drift [km/s]
MDC	32.4	—	272.7	+1.23	+33.4	+0.17	48.4	—
IMO 2012	32.5	28–35	272.6	+0.65	+33.2	−0.3	46.9	+0.25

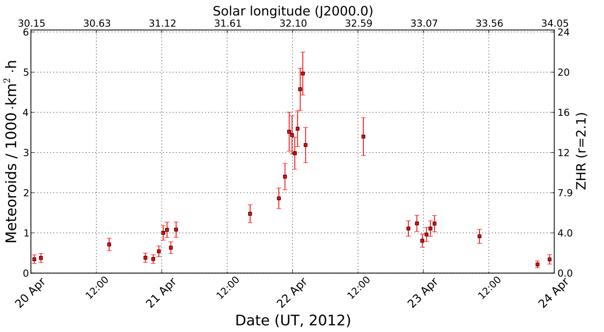

Figure 2 – Flux density profile of the Lyrids in 2012, based on 1 060 shower meteors.

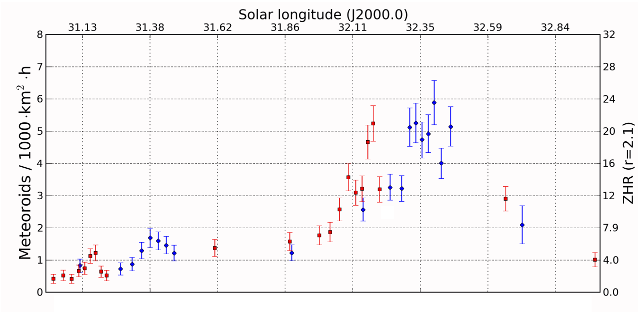

Figure 3 – Comparison of the Lyrid flux density profiles of 2011 (blue diamonds) and 2012 (red squares).

The quick look analysis at the IMO homepage yields a peak ZHR of 25 at 02^{h} UT on April 22 as well, based on 930 Lyrids (International Meteor Organization, 2012). That is a nice mutual confirmation of the results.

Just one year ago, we had inaugurated the video flux tool. On the occasion of the 2011 Lyrids, we measured for the first time the flux density of a meteor shower (Molau et al., 2011). Thus, we can now compare the results of two years for the first time. Figure 3 shows an overlay of the two profiles between 31° and 33° solar longitude. Up to a solar longitude of 32°, the activity graphs match quite well. Peak activity, however, occurred this year a little earlier than last year. Also that is in agreement with visual observations, which yielded a peak at 32.°2 solar longitude in 2011 (International Meteor Organization, 2011), about 0.°1 later than this year (International Meteor Organization, 2012).

Overall, the Lyrids are the most active radiant in their activity interval between April 18 and 25. The meteor shower parameters derived from 4 000 meteors (Table 1) have thus a high precision. It is interesting to see that the radiant position agrees very well with the values given in the meteor shower list of the IAU Meteor Data Center (MDC), but there is clear discrepancy in the radiant drift. As the individual radiants in our analysis show almost no scatter, we believe in the high precision of our values.

The Lyrids, however, are by far not the only meteor shower in April. In the following sections we want to discuss those additional five meteor showers from the MDC list (all with "working list" status), that could be traced in our data (whereby we disregard the Virginid complex this time).

3 ν-Cygnids

In our latest meteor shower analysis (Molau, 2012), there is a shower that can be traced over 31° in solar longitude between April 3 and May 5. More than 1 700 meteors were assigned to that shower, which is quite an amount for the meteor-wise weak spring time. A check with the MDC list revealed a good agreement with the ν-Cygnids (409 NCY). The large number is a hint that this shower was only recently detected, and a short investigation confirmed this result: That is one of the showers which we had detected in the IMO data during the last analysis in 2009 (Molau & Rendtel, 2009)!

Table 2 compares the shower parameters of 2009 with the current results. It is obvious that the shower can now be detected two weeks earlier thanks to the more than doubled data set, whereas the end date stays the same. Also the radiant position could be refined now. The activity of the shower remains weak in the full activity interval – highest rates were observed between April 21 and 30.

4 δ-Aquilids

Between April 7 and 13 we found the δ-Aquilids (131 DAL) with about 200 meteors. They show a uniform drift in right ascension and declination incident with a significant increase of the meteor shower velocity. All parameters are summarized in Table 3 and compared with the MDC values. Whereas there is a good match in right ascension and velocity, there is a deviation of more than 10° in declination. Still we believe that we are dealing with the same shower in both cases.

5 σ-Leonids

Also clearly detected in our data are the σ-Leonids (136 SLE) with more than 1 000 meteors from April 8 to 25. In particular in the first half of the month, this shower often presents the most active radiant in the night sky. Still, there are once more significant deviations between the parameters determined by us and the values from the MDC list (Table 4). However, from the MDC website it is not clear, from what data set the values are derived. Often the sources are much less reliable than the observations of the IMO Network which span more than a decade of video observations.

Table 2 – Parameters of the ν-Cygnids from the IMO Network analyses 2009 (Molau & Rendtel, 2009) and 2012 (this work).

Source	Solar Longitude		Right Ascension		Declination		V_∞	
	Mean [°]	Interval [°]	Mean [°]	Drift [°]	Mean [°]	Drift [°]	Mean [km/s]	Drift [km/s]
IMO 2009	30	28–44	305.2	+1.8	+39.4	+0.7	42	—
IMO 2012	28.5	13–44	310.5	+0.8	+43.2	+0.3	43.8	0.0

Table 3 – Parameters of the δ-Aquilids from the MDC Working List and the IMO Network analysis in 2012.

Source	Solar Longitude		Right Ascension		Declination		V_∞	
	Mean [°]	Interval [°]	Mean [°]	Drift [°]	Mean [°]	Drift [°]	Mean [km/s]	Drift [km/s]
MDC	23	—	310.6	—	−0.2	—	67.1	—
IMO 2012	20	17–23	308.0	+1.0	+11.7	+0.3	64.0	+0.5

Table 4 – Parameters of the σ-Leonids from the MDC Working List and the IMO Network analysis in 2012.

Source	Solar Longitude		Right Ascension		Declination		V_∞	
	Mean [°]	Interval [°]	Mean [°]	Drift [°]	Mean [°]	Drift [°]	Mean [km/s]	Drift [km/s]
MDC	27.7	—	192.6	—	+3.1	—	25.6	—
IMO 2012	26.5	18–35	201.1	+0.6	+2.7	0.0	21.6	−0.16

Table 5 – Parameters of the Southern May-Ophiuchids from the MDC Working List and the IMO Network analysis in 2012. The shower is split into two sections.

Source	Solar Longitude		Right Ascension		Declination		V_∞	
	Mean [°]	Interval [°]	Mean [°]	Drift [°]	Mean [°]	Drift [°]	Mean [km/s]	Drift [km/s]
MDC	56.7	—	258.0	—	−24.0	—	30.0	—
IMO 2012	41.5	25–58	233	+1.2	−13	−0.2	31.2	+0.15
IMO 2012	67	59–75	249	−0.1	−12	+0.5	26.3	−0.58

Table 6 – Parameters of the April χ-Librids from the MDC Working List and the IMO Network analysis in 2012.

Source	Solar Longitude		Right Ascension		Declination		V_∞	
	Mean [°]	Interval [°]	Mean [°]	Drift [°]	Mean [°]	Drift [°]	Mean [km/s]	Drift [km/s]
MDC	39	—	236.3	—	−18.9	—	36.0	—
IMO 2012	35.5	31–40	235.1	+0.5	−13.3	+0.4	36.2	—

6 Southern May-Ophiuchids

The Southern May-Ophiuchids (150 SOP) are maybe the most prominent shower beside the Lyrids. They can be traced between April 15 and June 6 with more than 5 000 shower members. There is no doubt that this shower is real, since starting from mid-May it is often the strongest radiant in the corresponding solar longitude interval. The question rather is whether this is indeed just one shower, or two or more showers nearby respectively merging into one another. The shower pops up, remains active for a few days, disappears almost completely only to return one day later slightly displaced. If the radiant drift is visualized over the full activity interval, it can be split into two segments. There is no break in activity at the reversal point around May 20 (59° solar longitude), but both the drift in right ascension and declination changes that day, and even the rate of velocity change. Thus, both sections of the Southern May-Ophiuchids are given separately in Table 5.

7 April χ-Librids

Finally we want to list the less prominent April χ-Librids (140 XLI). They are present between April 21 and May 1 with about 500 shower meteors. The April χ-Librids never dominate meteor shower activity at any time, but still show only a relative small scatter in their parameters (Table 6). There is a also reasonable agreement with the MDC values.

References

International Meteor Organization (2011). "Lyrids 2011: visual data quicklook". `http://www.imo.net/live/lyrids2011` .

International Meteor Organization (2012). "Lyrids 2012: visual data quicklook". `http://www.imo.net/live/lyrids2012` .

Molau S. (2012). "Million Meteors in the IMO Video Meteor Database". `http://www.imonet.org/radiants/` .

Molau S., Kac J., Berko E., Crivello S., Stomeo E., Igaz A., and Barentsen G. (2011). "Results of the IMO Video Meteor Network – April 2011". *WGN, Journal of the IMO*, **39:4**, 100–104.

Molau S. and Rendtel J. (2009). "A Comprehensive List of Meteor Showers Obtained from 10 Years of Observations with the IMO Video Meteor Network". *WGN, Journal of the IMO*, **37:4**, 98–121.

Handling Editor: Javor Kac

Table 7 – Observers contributing to 2012 April data of the IMO Video Meteor Network. Eff.CA designates the effective collection area.

Code	Name	Place	Camera	FOV [°²]	Stellar LM [mag]	Eff.CA [km²]	Nights	Time [h]	Meteors
ARLRA	Arlt	Ludwigsfelde/DE	Ludwig1 (0.8/8)*	1488	4.8	726	11	62.0	34
BERER	Berko	Ludányhalászi/HU	Hulud1 (0.95/3)	2256	4.8	1540	13	69.1	244
			Hulud2 (0.75/6)	4860	3.9	1103	13	46.6	120
			Hulud3 (0.75/6)	4661	3.9	1052	13	43.0	110
BREMA	Breukers	Hengelo/NL	Mbb3 (0.75/6)	2399	4.2	699	11	45.9	84
			Mbb4 (0.8/8)	1470	5.1	1208	11	45.3	67
BRIBE	Brinkmann	Herne/DE	Hermine (0.8/6)	2374	4.2	678	14	50.1	82
		Bergisch Gladbach/DE	Klemoi (0.8/6)	2286	4.6	1080	17	54.7	94
CRIST	Crivello	Valbrevenna/IT	Bilbo (0.8/3.8)	5458	4.2	1772	19	89.5	217
			C3P8 (0.8/3.8)	5455	4.2	1586	18	83.1	154
			Stg38 (0.8/3.8)	5614	4.4	2007	21	87.9	220
CSISZ	Csizmadia	Zalaegerszeg/HU	Huvcse01 (0.95/5)	2423	3.4	361	15	66.5	134
ELTMA	Eltri	Venezia/IT	Met38 (0.8/3.8)	5631	4.3	2151	12	71.5	200
GONRU	Goncalves	Tomar/PT	Templar1 (0.8/6)	2179	5.3	1842	10	65.3	210
			Templar2 (0.8/6)	2080	5.0	1508	13	87.7	226
			Templar3 (0.8/8)	1438	4.3	571	21	117.6	141
GOVMI	Govedič	Središče ob Dravi/SI	Orion2 (0.8/8)	1447	5.5	1841	21	150.8	388
			Orion3 (0.95/5)	2665	4.9	2069	20	120.8	103
			Orion4 (0.95/5)	2662	4.3	1043	22	146.8	191
HINWO	Hinz	Brannenburg/DE	Acr (2.0/35)*	557	7.4	4954	14	56.8	323
IGAAN	Igaz	Baja/HU	Hubaj (0.8/3.8)	5552	2.8	403	22	63.9	166
		Debrecen/HU	Hudeb (0.8/3.8)	5522	3.2	620	21	139.2	199
		Hódmezővásárhely/HU	Huhod (0.8/3.8)	5502	3.4	764	22	132.6	175
		Budapest/HU	Hupol (1.2/4)	3790	3.3	475	16	72.9	43
		Sopron/HU	Husop (0.8/6)	2031	3.8	460	26	154.8	499
JONKA	Jonas	Budapest/HU	Husor (0.95/4)	2286	3.9	445	18	113.3	87
KACJA	Kac	Kostanjevec/SI	Metka (0.8/8)*	1372	4.0	361	8	58.4	77
		Ljubljana/SI	Orion1 (0.8/8)	1402	3.8	331	18	102.0	149
		Kamnik/SI	Cvetka (0.8/3.8)	4914	4.3	1842	11	72.1	164
			Rezika (0.8/6)	2270	4.4	840	16	90.8	338
KERST	Kerr	Glenlee/AU	Gocam1 (0.8/3.8)	5189	4.6	2550	29	179.3	988
KOSDE	Koschny	Izana Obs./ES	Icc7 (0.85/25)*	714	5.9	1464	14	59.9	388
		Noordwijkerhout/NL	Lic4 (1.4/50)*	2027	6.0	4509	14	57.5	121
LERAR	Leroy	Gretz/FR	Saphira (1.2/6)	3260	3.4	301	14	88.9	35

Table 7 – Observers contributing to 2012 April data of the IMO Video Meteor Network – continued from previous page.

Code	Name	Place	Camera	FOV [°2]	Stellar LM [mag]	Eff.CA [km2]	Nights	Time [h]	Meteors
MACMA	Maciejewski	Chelm/PL	Pav35 (1.2/4)	4383	2.5	253	17	73.1	53
			Pav36 (1.2/4)*	5732	2.2	227	14	70.9	103
			Pav43 (0.95/3.75)*	2544	2.7	176	15	79.5	75
MARGR	Maravelias	Lofoupoli-Crete/GR	Loomecon (0.8/12)	738	6.3	2698	19	118.1	276
MOLSI	Molau	Seysdorf/DE	Avis2 (1.4/50)*	1776	6.1	3817	12	62.0	411
			Mincam1 (0.8/8)	1477	4.9	1084	21	110.1	189
		Ketzür/DE	Remo1 (0.8/8)	1467	6.0	3139	25	137.2	522
			Remo2 (0.8/8)	1475	5.6	1965	22	120.7	216
OCAFR	Ocaña Gonzáles	Madrid/ES	Fogcam (1.4/8)	1890	3.9	109	14	78.0	69
OCHPA	Ochner	Albiano/IT	Albiano (1.2/4.5)	1971	—	—	8	25.6	49
OTTMI	Otte	Pearl City/US	Orie1 (1.4/5.7)	3837	3.8	460	24	92.2	216
PERZS	Perko	Becsehely/HU	Hubec (0.8/3.8)*	5498	2.9	460	18	108.4	373
PUCRC	Pucer	Nova vas nad Dragonjo/SI	Mobcam1 (0.75/6)	2398	5.3	2976	21	92.7	173
ROTEC	Rothenberg	Berlin/DE	Armefa (0.8/6)	2366	4.5	911	16	61.0	93
SARAN	Saraiva	Carnaxide/PT	Ro1 (0.75/6)	2362	3.7	381	15	70.3	75
			Ro2 (0.75/6)	2381	3.8	459	19	78.2	95
			Sofia (0.8/12)	738	5.3	907	17	79.4	62
SCALE	Scarpa	Alberoni/IT	Leo (1.2/4.5)*	4152	4.5	2052	18	66.8	170
SCHHA	Schremmer	Niederkrüchten/DE	Doraemon (0.8/3.8)	4900	3.0	409	16	69.4	78
SLAST	Slavec	Ljubljana/SI	Kayak1 (1.8/28)	588	—	—	7	10.6	31
STOEN	Stomeo	Scorze/IT	Min38 (0.8/3.8)	5566	4.8	3270	16	79.4	398
			Noa38 (0.8/3.8)	5609	4.2	1911	15	72.3	197
			Sco38 (0.8/3.8)	5598	4.8	3306	16	83.2	251
STORO	Stork	Kunzak/CZ	Kun1 (1.4/50)*	1913	5.4	2778	3	18.6	220
		Ondrejov/CZ	Ond1 (1.4/50)*	2195	5.8	4595	3	16.5	234
STRJO	Strunk	Herford/DE	Mincam2 (0.8/6)	2362	4.6	1152	7	33.1	35
			Mincam3 (0.8/12)	728	5.7	975	13	57.0	61
			Mincam4 (1.0/2.6)	9791	2.7	552	8	34.4	21
			Mincam5 (0.8/6)	2349	5.0	1896	15	65.4	92
TEPIS	Tepliczky	Budapest/HU	Humob (0.8/6)	2388	4.8	1607	21	131.7	368
TRIMI	Triglav	Velenje/SI	Sraka (0.8/6)*	2222	4.0	546	19	55.1	154
YRJIL	Yrjölä	Kuusankoski/FI	Finexcam (0.8/6)	2337	5.5	3574	21	64.5	177
						Overall	30	5 262.0	12 208

* active field of view smaller than video frame

Results of the IMO Video Meteor Network — May 2012

Sirko Molau[1], *Javor Kac*[2], *Erno Berko*[3], *Stefano Crivello*[4], *Enrico Stomeo*[5], *Antal Igaz*[6] *and Geert Barentsen*[7]

Preliminary results for 2012 May observations of the IMO Video Meteor Network cameras is presented, obtained by 40 observers using 73 video systems. More than 15 000 meteors were recorded in almost 6 000 hours of effective observing time. The flux density profiles of η-Aquariids and η-Lyrids are presented. Details on StrmFind tool improvement are presented and χ-Capricornid shower parameters refined.

Received 2012 July 3

1 Introduction

The weather in May was not as perfect this year as in 2011, but it was still a fruitful month for the video observers which were more numerous than ever before. Overall 40 observers contributed with 73 video systems to the IMO Video Meteor Network. Half of the systems recorded meteors in twenty or more nights, so that the effective observing time grew to almost 6 000 hours. The average meteor activity, however, was slightly below the value of the previous year (2.5 instead of 3.1 meteors per hour) which is why the total number of 15 000 meteors almost matched the result of May 2011 (Molau et al., 2011). Table 2 and Figure 1 summarize the May 2012 results.

Also in May the camera network could be extended. With Hungarian Zsofia Biro the second female observer joined our forces. Zsofia's camera Huago started to operate in late November 2011, but first some configuration issues had to be fixed. Now all observations are included in the IMO Video Meteor database.

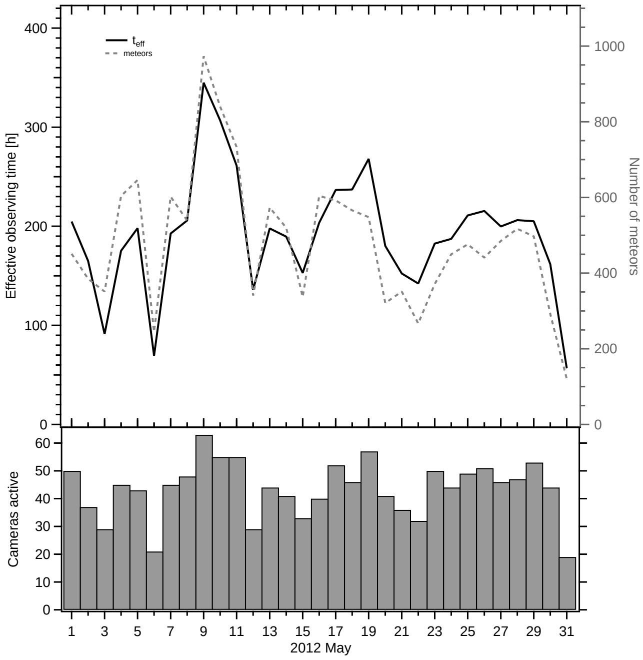

Figure 1 – Monthly summary for the effective observing time (solid black line), number of meteors (dashed gray line) and number of cameras active (bars) in 2012 May.

2 η-Aquariids

With respect to meteor showers, May was once more dominated by the η-Aquariids. Among other, also this shower yielded our Australian observer Steve Kerr a respectable total of almost 2 000 meteors. But also the northern hemisphere observers caught one or the other shower member in early May.

In Australia, the radiant lies 60° below the horizon in the evening hours, but rises to more than 50° above the horizon at dawn. In the shorter European nights, the radiant starts the night at 40° below the horizon, and even at more southern observing sites it hardly reaches 20° altitude in the morning hours. Almost no other shower exhibits such tremendous altitude variations as the η-Aquariids, which is why the zenith exponent (or comparable effects) have a strong impact. So the original flux density profile based on more than 1 000 η-Aquariids (with 11 800 sporadic meteors at the same time) shows the typical variations, which reduce significantly when a zenith exponent of 1.6 is applied (Figure 2). However, with the zenith exponent also the peak density raises from 30 (zenith exponent 1.0) to over 60 (zenith exponent 1.6) meteoroids per 1 000 km^2 per hour.

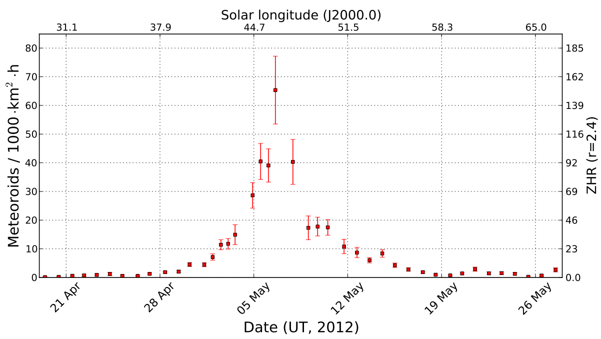

Figure 2 – Flux density profile of the η-Aquariids in May 2012, obtained with a zenith exponent of 1.6.

[1]Abenstalstr. 13b, 84072 Seysdorf, Germany. Email: sirko@molau.de

[2]Na Ajdov hrib 24, 2310 Slovenska Bistrica, Slovenia. Email: javor.kac@orion-drustvo.si

[3]Bercsenyi ut 3, 3188 Ludanyhalaszi, Hungary. Email: berko@is.hu

[4]Via Bobbio 9a/18, 16137 Genova, Italy. Email: stefano.crivello@libero.it

[5]via Umbria 21/d, 30037 Scorze (VE), Italy. Email: stom@iol.it

[6]Húr u. 9/D, H-1223 Budapest, Hungary. Email: antaligaz@yahoo.com

[7]University of Hertfordshire, Hatfield AL10 9AB, United Kingdom. Email: geert@barentsen.be

IMO bibcode WGN-404-molau-vidmay
NASA-ADS bibcode 2012JIMO...40..144M

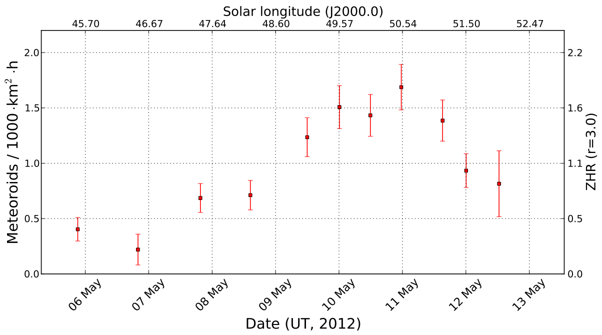

Figure 3 – Flux density profile of the η-Lyrids in May 2012.

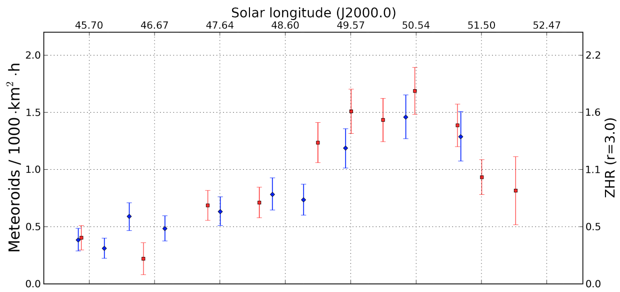

Figure 4 – Comparison of the η-Lyrid flux density profiles of 2011 (blue diamonds) and 2012 (red squares).

3 η-Lyrids

The second shower of the IMO Working List are the η-Lyrids. They are active around May 10 and could be covered well by our video cameras. Figure 3 shows the flux density profile of this shower, determined from more than 400 shower members (with 2 600 sporadics in parallel). The flux density hardly reaches a value of two meteoroids per 1 000 km^2 per hour, which gives a peak ZHR of the same value. So this shower will not thrill any visual observer.

Also in this case, we find a good agreement in the flux density profiles of 2011 and 2012 between 45° and 53° solar longitude (Figure 4).

4 StrmFind tool improvements

As announced in April report (Molau et al., 2012), we generated a new list of radiants per solar longitude interval and published it on the internet. Thus, everybody can verify his own meteor shower hypothesis with our data. In the last few days, the StrmFind tool, which is used to automatically extract meteor showers from the radiant list, was reworked. There were basically four changes.

The first modification was about the tracking of radiants. So far, meteor showers were determined "left to right". That is, new radiants we linked to existing radiant chains synchronously with increasing solar longitude. In particular at the beginning of showers, their activity is weak and the radiant position poorly determined, which is why there is a risk that wrong radiants are linked and that the raising edge of showers is less accurate.

The new procedure searches "forward–backward". At first, the strongest not yet assigned radiant is determined over all solar longitudes. For this radiant, the extension is searched for forward and backward in solar longitude. If no further extension is possible, the next strongest unassigned radiant is determined and the procedure is repeated iteratively.

A comparison shows that both methods yield identical results at higher meteor shower activity, but the results differ at lower activity. The old procedure sometimes has problems with the onset of a meteor shower as described. In case of nearby showers such as the Taurids, however, the new procedure may lead to "cannibalization" among the showers.

The second change was the newly introduces rank of a shower. The rank of a radiant describes at which position it is located in the sorted radiant list of that solar longitude interval. The rank of a meteor shower is the median rank of the individual radiant belonging to it. That value is useful to distinguish between real showers and chance alignments of radiants. In case of a shower with rank five, for example, the radiant was most of the time among the most active sources in the sky and the shower is real with a high confidence. Also if the rank is ten, chances are good that it is a real shower, whereas a rank above fifteen may well be a chance alignment of weak radiants.

The third change relates to the MDC meteor shower list, which was updated in the software.

Last but not least, an optional parameter was introduced that outputs the result not only in text, but also in HTML format ready for internet publishing.

The result of the new software was made available online at `http://www.imonet.org/showers`. One can see there which meteor shower candidates were extracted from the radiant list, and how well they possibly fit to a MDC meteor shower. Note that there was no manual clean up or verification of the resulting list!

4.1 χ-Capricornids

Beside the η-Aquariids, η-Lyrids and the minor showers presented in the last reports, the χ-Capricornids (76 CCA) were identified, for example. With a rank of 13, this shower falls into the borderline category. However, checking the individual radiants there is almost no fluctuation in position and velocity between 56° and 61° solar longitude. Hence, even if the activity is very low, this shower seems to be real (Table 1). For more details, please refer to the online shower list mentioned above.

References

Molau S., Kac J., Berko E., Crivello S., Stomeo E., Igaz A., and Barentsen G. (2011). "Results of the IMO Video Meteor Network – May 2011". *WGN, Journal of the IMO*, **39:4**, 105–109.

Molau S., Kac J., Berko E., Crivello S., Stomeo E., Igaz A., and Barentsen G. (2012). "Results of the IMO Video Meteor Network – April 2012". *WGN, Journal of the IMO*, **40:4**, 139–143.

Handling Editor: Javor Kac

Table 1 – Parameters of the χ-Capricornids from the MDC Working List and the analysis of the IMO Network in 2012.

Source	Solar Longitude		Right Ascension		Declination		V_∞ [km/s]	
	Mean	Interval	Mean	Drift	Mean	Drift	Mean	Drift
MDC	58°	—	314.°3	—	−23.°2	—	66.3	—
IMO 2012	58.°5	56°–61°	304.°4	+0.°7	−15.°3	+0.°3	68	—

Figure 5 – This fireball of apparent magnitude −7/−8 was filmed by 3 Italian videocameras. The fireball traveled the first part of the luminous trajectory of 59-km in about 3.9 s over North Italy (Emilia Romagna area). The following results are preliminary: beginning of luminous trajectory 86 km above 44.°6 N, 11.°4 E, end 35 km above 44.°6 N, 11.°7 E, observed radiant $\alpha = 233.°4$, $\delta = +40.°9$ (eq.2000). Orbit: $a = 1.34$ AU, $q = 0.95$ AU, $e = 0.29$, $\omega = 222.°0$, $\Omega = 44.°8$, $i = 14.°3$ (eq.2000). Feft image: FERse, operated by F. Zanotti (IMTN); right image: MET38, operated by E. Stomeo (UAI-SM).

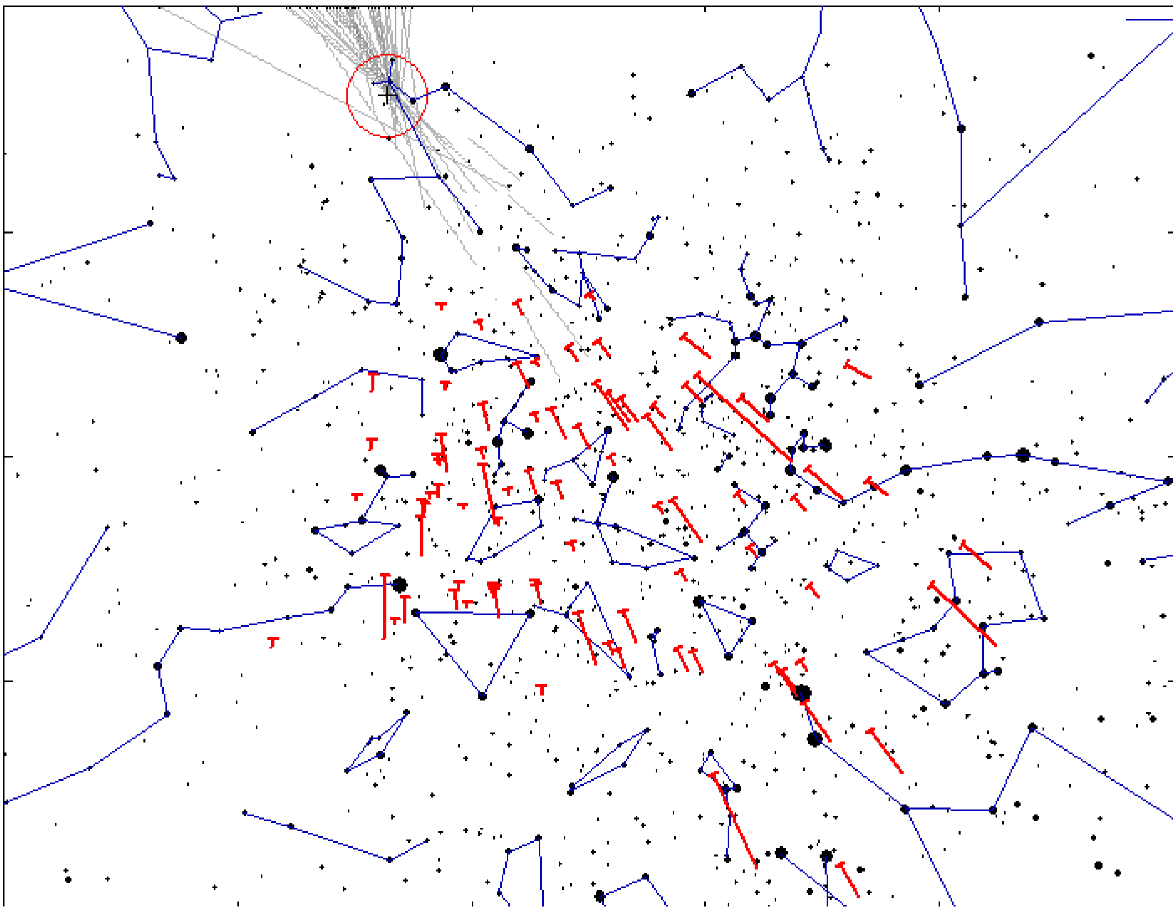

Figure 6 – Backward tracing plot based on 81 η-Aquariids recorded on 2012 May 5 with Gocam1 camera operated by Steve Kerr. The η-Aquariid radiant is marked by circle. Image courtesy: Stefano Crivello.

Table 2 – Observers contributing to 2012 May data of the IMO Video Meteor Network. Eff.CA designates the effective collection area.

Code	Name	Place	Camera	FOV [°2]	Stellar LM [mag]	Eff.CA [km²]	Nights	Time [h]	Meteors
ARLRA	Arlt	Ludwigsfelde/DE	Ludwig1 (0.8/8)*	1488	4.8	726	8	36.3	31
BASLU	Bastiaens	Hove/BE	Urania1 (0.8/3.8)*	4545	2.5	237	3	5.8	4
BERER	Berko	Ludányhalászi/HU	Hulud1 (0.95/3)	2256	4.8	1540	14	65.8	206
			Hulud2 (0.75/6)	4860	3.9	1103	14	53.2	135
			Hulud3 (0.75/6)	4661	3.9	1052	13	43.1	94
BIRSZ	Biro	Agostyán/HU	Huago (0.75/4.5)	2427	4.4	1036	26	126.3	200
BOMMA	Bombardini	Faenza/IT	Mario (1.2/4.0)	5794	3.3	739	24	112.9	299
BREMA	Breukers	Hengelo/NL	Mbb3 (0.75/6)	2399	4.2	699	16	60.6	75
			Mbb4 (0.8/8)	1470	5.1	1208	16	53.3	53
BRIBE	Brinkmann	Herne/DE	Hermine (0.8/6)	2374	4.2	678	22	94.2	178
		Bergisch Gladbach/DE	Klemoi (0.8/6)	2286	4.6	1080	25	100.1	151
CASFL	Castellani	Monte Baldo/IT	Bmh1 (0.8/6)	2350	5.0	1611	18	54.3	165
			Bmh2 (1.5/4.5)*	4243	3.0	371	20	56.0	160
CRIST	Crivello	Valbrevenna/IT	Bilbo (0.8/3.8)	5458	4.2	1772	24	116.0	298
			C3P8 (0.8/3.8)	5455	4.2	1586	21	85.8	179
			Stg38 (0.8/3.8)	5614	4.4	2007	24	102.5	339
CSISZ	Csizmadia	Zalaegerszeg/HU	Huvcse01 (0.95/5)	2423	3.4	361	19	43.1	95
ELTMA	Eltri	Venezia/IT	Met38 (0.8/3.8)	5631	4.3	2151	20	92.4	203
GONRU	Goncalves	Tomar/PT	Templar1 (0.8/6)	2179	5.3	1842	18	103.5	280
			Templar2 (0.8/6)	2080	5.0	1508	17	113.8	243
			Templar3 (0.8/8)	1438	4.3	571	26	144.0	184
GOVMI	Govedič	Središče ob Dravi/SI	Orion2 (0.8/8)	1447	5.5	1841	19	101.3	243
			Orion3 (0.95/5)	2665	4.9	2069	16	40.4	70
			Orion4 (0.95/5)	2662	4.3	1043	17	77.1	128
HINWO	Hinz	Brannenburg/DE	Acr (2.0/35)*	557	7.4	4954	14	49.2	277
IGAAN	Igaz	Baja/HU	Hubaj (0.8/3.8)	5552	2.8	403	19	74.2	143
		Debrecen/HU	Hudeb (0.8/3.8)	5522	3.2	620	23	123.0	180
		Hódmezővásárhely/HU	Huhod (0.8/3.8)	5502	3.4	764	22	118.9	164
		Budapest/HU	Hupol (1.2/4)	3790	3.3	475	17	67.9	55
		Sopron/HU	Husop (0.8/6)	2031	3.8	460	27	112.0	350
JONKA	Jonas	Budapest/HU	Husor (0.95/4)	2286	3.9	445	23	103.2	143
KACJA	Kac	Kostanjevec/SI	Metka (0.8/8)*	1372	4.0	361	8	42.7	53
		Ljubljana/SI	Orion1 (0.8/8)	1402	3.8	331	21	100.9	155
		Kamnik/SI	Cvetka (0.8/3.8)	4914	4.3	1842	13	64.2	191
			Rezika (0.8/6)	2270	4.4	840	16	78.4	356
			Stefka (0.8/3.8)	5471	2.8	379	9	44.0	64
KERST	Kerr	Glenlee/AU	Gocam1 (0.8/3.8)	5189	4.6	2550	29	248.0	1904

Table 2 – Observers contributing to 2012 May data of the IMO Video Meteor Network – continued from previous page.

Code	Name	Place	Camera	FOV [°2]	Stellar LM [mag]	Eff.CA [km^2]	Nights	Time [h]	Meteors
KOSDE	Koschny	Izana Obs./ES	Icc7 (0.85/25)*	714	5.9	1464	25	173.5	1106
		Noordwijkerhout/NL	Lic4 (1.4/50)*	2027	6.0	4509	13	44.5	108
LERAR	Leroy	Gretz/FR	Saphira (1.2/6)	3260	3.4	301	9	45.7	23
MACMA	Maciejewski	Chelm/PL	Pav35 (1.2/4)	4383	2.5	253	21	77.9	55
			Pav36 (1.2/4)*	5732	2.2	227	13	42.5	54
			Pav43 (0.95/3.75)*	2544	2.7	176	20	61.0	84
MARGR	Maravelias	Lofoupoli-Crete/GR	Loomecon (0.8/12)	738	6.3	2698	29	155.3	298
MOLSI	Molau	Seysdorf/DE	Avis2 (1.4/50)*	1776	6.1	3817	20	90.3	613
			Mincam1 (0.8/8)	1477	4.9	1084	27	132.3	252
		Ketzür/DE	Remo1 (0.8/8)	1467	6.0	3139	24	106.9	450
			Remo2 (0.8/8)	1475	5.6	1965	23	104.4	201
MORJO	Morvai	Fülöpszállás/HU	Huful (1.4/5)	2522	3.5	532	23	104.0	128
OCAFR	Ocaña Gonzáles	Madrid/ES	Fogcam (1.4/7)	1890	3.9	109	16	42.0	88
OCHPA	Ochner	Albiano/IT	Albiano (1.2/4.5)	2944	3.5	357	18	57.2	113
OTTMI	Otte	Pearl City/US	Orie1 (1.4/5.7)	3837	3.8	460	24	105.9	235
PERZS	Perko	Becsehely/HU	Hubec (0.8/3.8)*	5498	2.9	460	25	127.2	365
PUCRC	Pucer	Nova vas nad Dragonjo/SI	Mobcam1 (0.75/6)	2398	5.3	2976	16	65.8	166
ROTEC	Rothenberg	Berlin/DE	Armefa (0.8/6)	2366	4.5	911	3	11.1	18
SARAN	Saraiva	Carnaxide/PT	Ro1 (0.75/6)	2362	3.7	381	21	120.1	144
			Ro2 (0.75/6)	2381	3.8	459	21	119.3	136
			Sofia (0.8/12)	738	5.3	907	18	87.9	68
SCALE	Scarpa	Alberoni/IT	Leo (1.2/4.5)*	4152	4.5	2052	18	81.5	176
SCHHA	Schremmer	Niederkrüchten/DE	Doraemon (0.8/3.8)	4900	3.0	409	21	90.8	100
SLAST	Slavec	Ljubljana/SI	Kayak1 (1.8/28)	588	—	—	17	28.8	55
STOEN	Stomeo	Scorze/IT	Min38 (0.8/3.8)	5566	4.8	3270	20	100.4	375
			Noa38 (0.8/3.8)	5609	4.2	1911	21	99.2	318
			Sco38 (0.8/3.8)	5598	4.8	3306	20	103.6	411
STORO	Stork	Kunzak/CZ	Kun1 (1.4/50)*	1913	5.4	2778	3	4.5	27
		Ondrejov/CZ	Ond1 (1.4/50)*	2195	5.8	4595	4	7.2	66
STRJO	Strunk	Herford/DE	Mincam2 (0.8/6)	2362	4.6	1152	18	66.3	69
			Mincam3 (0.8/12)	728	5.7	975	21	55.9	67
			Mincam4 (1.0/2.6)	9791	2.7	552	15	60.7	35
			Mincam5 (0.8/6)	2349	5.0	1896	23	79.2	118
TEPIS	Tepliczky	Budapest/HU	Humob (0.8/6)	2388	4.8	1607	25	116.7	298
TRIMI	Triglav	Velenje/SI	Sraka (0.8/6)*	2222	4.0	546	19	45.5	138
YRJIL	Yrjölä	Kuusankoski/FI	Finexcam (0.8/6)	2337	5.5	3574	10	13.0	32
						Sum	30	5 936.7	15 038

* active field of view smaller than video frame

The International Meteor Organization

web site `http://www.imo.net`

IMO Sales

Available from the Treasurer or the Electronic Shop on the IMO Website	€	$
IMO membership, including subscription to WGN Vol. 40 (2012)		
Surface mail	26	39
Air Mail (outside Europe only)	49	69
Electronic subscription only	21	29
Back issues of WGN on paper (price per complete volume)		
Vols. 26 (1998) – 35 (2007) except 30 (2002), 38 (2010), 39 (2011)	15	23
Vols. 37 (2009) – 39 (2011) – electronic version only	9	13
Proceedings of the International Meteor Conference on paper		
1990, 1991, 1993, 1995, 1996, 1999, 2000, 2002, 2003, per year	9	13
2007, 2009, 2010	15	23
Proceedings of the Meteor Orbit Determination Workshop 2006	15	23
Proceedings of the Radio Meteor School 2005 on paper	15	23
Handbook for Meteor Observers	20	29
Electronic media		
Meteor Beliefs Project CD-ROM	5	7
DVD: WGN Vols. 6–30 & IMC 1991, 1993–96, 2001–04	45	69

Fireballs from Slovenia

A handful of fireballs were captured on 2012 August 12/13 simultaneously by Cvetka (3.8 mm $f/0.8$ lens) operating at Rezman Observatory, Slovenia (left column), and by Mobcam1 (6 mm $f/0.75$ lens) operating at SMART youth astronomical research camp in Medvedje Brdo, Slovenia (right column). Photos courtesy of Javor Kac and Rok Pucer.

Sporadic magnitude −6 fireball with a double flare at $22^{\mathrm{h}}12^{\mathrm{m}}14^{\mathrm{s}}$ UT.

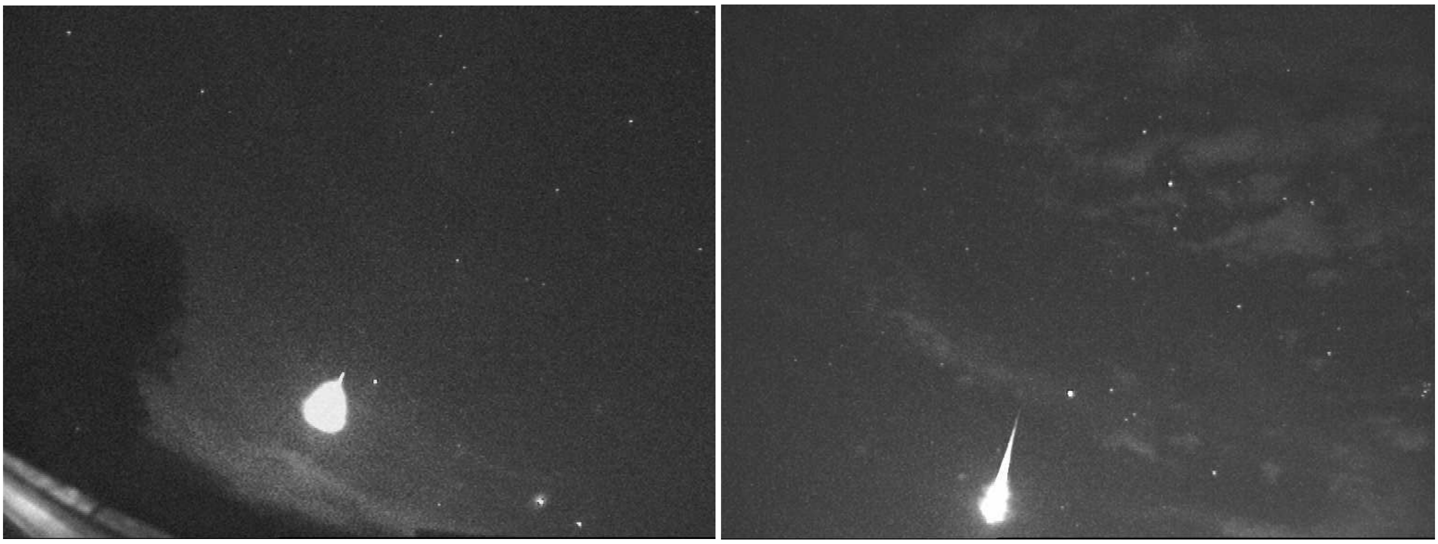

Magnitude −7 Perseid fireball at $00^{\mathrm{h}}35^{\mathrm{m}}37^{\mathrm{s}}$ UT.

Magnitude −5 Perseid fireball at $01^{\mathrm{h}}34^{\mathrm{m}}57^{\mathrm{s}}$ UT.